Angewandte Chemie
Eine Zeitschrift der Gesellschaft Deutscher Chemiker

Supporting Information

Expanding the Molecular Switches Toolbox: Photoreloadable Dithienylethene Mechanophores

M. Steponavičiūtė, D. Majee, B. Zhao, L. Ungur, S. Presolski**

Supporting Information

Expanding the Molecular Switches Toolbox: Photoreloadable Dithienylethene Mechanophores

Medeina Steponavičiūtė[1], Debashis Majee[1], Bisheng Zhao[2], Liviu Ungur[2], Stanislav Presolski[1,3]
[1] Chemical and Biomolecular Engineering, CDE, NUS
[2] Department of Chemistry, FOS, NUS
[3] Yale-NUS College, NUS
yncpsi@nus.edu.sg

Table of Contents

1. General Information *S2*
Procedure for the sonication *S2*
Photochemistry of 2,2'-diOAc and 5,5'-diOAc. *S3*
Compound Solution Preparation *S3*
Computational Details *S9*
2. Synthesis *S12*
Polymerization of ε-Caprolactone (PCL) with 2,2'-diOH and 5,5'-diOH DTE *S12*
Poly(ε-caprolactone) synthesis *S12*
Synthesis procedure of 2,2'-diOAc *S16*
Synthesis procedure of 5,5'-diOAc. *S20*
3. Measurements and Analysis *S34*
References*:* *S42*

1. General Information

All reagents and solvents were obtained from Sigma-Aldrich and, unless otherwise stated, were used without further purification. Tin(II) 2-ethylhexanoate ($Sn(Oct)_2$, 98%, Aldrich) in 1-butanol (99.8%, anhydrous, Aldrich) was stirred overnight with anhydrous magnesium sulfate (Aldrich) and distilled. ε-Caprolactone (99%, Aldrich) was dried over calcium hydride and purified by distillation under reduced pressure, then stored under nitrogen. Toluene was distilled over calcium hydride (CaH_2) and stored over 3Å molecular sieve. Ultrasound experiments were performed using a Qsonica Q125 Sonicator with 1 second ON and 1 second OFF duty cycles in 1,4-dioxane, using an ice bath to maintain solution at constant temperature. Ultraviolet-visible (UV-Vis) spectra were recorded on a portable Vernier Ocean Optics™ spectrophotometer or on an Agilent Technologies Cary 60. Computational calculation and simulations were performed using the ORCA computational package, employing the XTB22 method. Full details and data analysis methodology can be found in Supplementary Information.

^1H NMR spectra were recorded at 23 °C using Bruker 400 Ascend™ nuclear magnetic resonance spectrometer (400 MHz) in $CDCl_3$.

Gel permeation chromatography (GPC) was used to characterize DTE-PCL polymers. Measurements were carried out at 30 °C with Agilent 1200 HPLC-GPC System. Tetrahydrofuran (THF) was used as the eluent at a flow rate of 1 mL/min. The SEC system was calibrated, and molecular weights were determined based on molecular weight polystyrene calibration (from 162 to 91450 g/mol).

Ultraviolet-visible (UV-Vis) spectra were recorded on Ocean Optics™, a portable Vernier Vis-NIR Spectrometer, over a range of 380–950 nm or on Agilent Technologies Cary 60 spectrophotometer in 10mm Latech Scientific quartz cuvettes.

Sonication experiments were performed by a Qsonica Q125 Sonicator Ultrasonic Homogenizer (figure S1) equipped with a 0.3 cm diameter solid probe. An ice bath was used to maintain a constant solution temperature ~ of 15 - 20 ˚C during the experiments. The distance between the titanium tip and the bottom of the sample bottle was 0.5 cm.

Procedure for the sonication

The DTE with polymer chains was dissolved in 1,4-dioxane by leaving overnight. Before the measurements, the solution was exposed to 311 nm UV radiation for 2 min when the polymer with 2,2'-DTE or 1.5 min when the polymer with 5,5'-DTE chromophore group. The bottle with the polymer solution was then immersed in the ice bath and put under the pulsed ultrasonication with on and of periods - 1 s on, 1 s off, and output intensity set at 50%, with an internal temperature fluctuating

between 15 - 20°C. After a certain amount of time, the aliquots of 1.5 ml were removed and transferred to the cell, and the absorption spectra of the samples were recorded with a spectrometer. After the measurement sample was returned to the bottle and ultrasonication was continued. The same procedure is repeated at set time intervals until the experiment is completed. Ultracentrifugation experiment is performed in a closed, blind box to protect against daylight effect.

Figure S1. Ultrasonification system.

Photochemistry of 2,2′-diOAc and 5,5′-diOAc.

Compound Solution Preparation

3.6 mg of **2,2′-diOAc** and 3.07 mg of **5,5′-diOAc** were separately dissolved in 10 mL of HPLC-grade dioxane to make stock solutions of 700 µM and 600 µM respectively for UV and HPLC measurements. 1.0 mg of 4,4-dimethyl-2-(5-(4-nitrophenyl)thiophen-2-yl)-4,5-dihydrooxazole was dissolved in 10 ml of HPLC grade acetonitrile to make 0.36 mM solution for the use of reference in HPLC run. The stock solutions were stored at 4 °C to prevent evaporation and were exposed to white light before use to counteract the effect of any stray UV light from fluorescent tube lighting.

Light Sources

The UV irradiation was performed using a 311 nm Philips UV lamp delivering 2 mW/cm^2 (measured by ThorLabs power meter) at the base of the standard 10x10 mm cuvette. An iPhone 14 Pro flashlight provided visible light with power of 115 mW. The light-sensitive experiments were conducted in a dark room with a small LED torch covered with a red filter (transmission >650 nm).

UV-Vis Measurements

First, 1.5 mL of **2,2′-diOAc** solution was added to a quartz cuvette. The solution was then exposed to 311 nm UV light for 2 minutes, ensuring the light source was optimally aligned and positioned for maximum photon absorption. Afterward, 500 µL of the exposed solution was mixed with 1.0 mL of dioxane in another quartz cuvette, and the UV-vis spectrum was measured. The diluted solution was

then exposed to visible light at short intervals, and the UV-vis spectrum was measured repeatedly until the band disappeared in the visible region.

For the **5,5′-diOAc** solution, the same procedure was followed for UV measurement, but the irradiation of UV light duration was 1.5 minutes instead of 2 minutes.

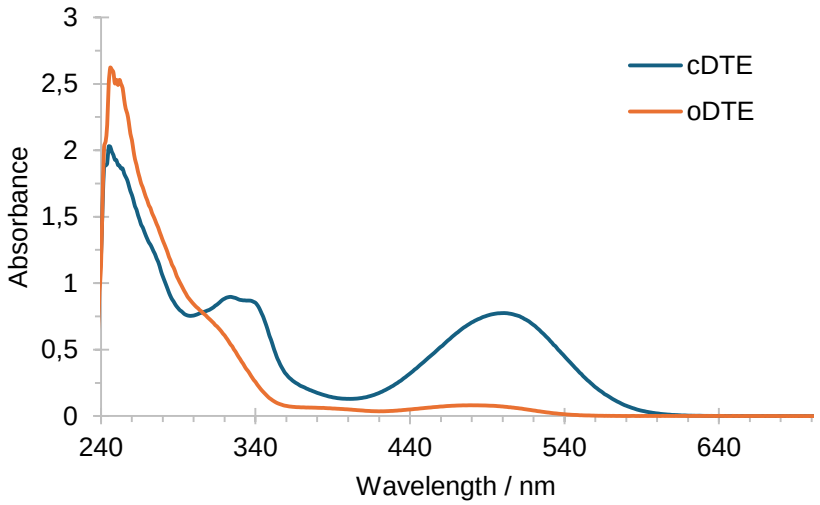

Figure S2. UV absorption spectra of 233 µM **2,2′-diOAc** upon irradiation of 700 µM stock solution in dioxane with 311 nm light for 2 min. (blue line), followed by irradiation with visible light for 10 min. (orange line).

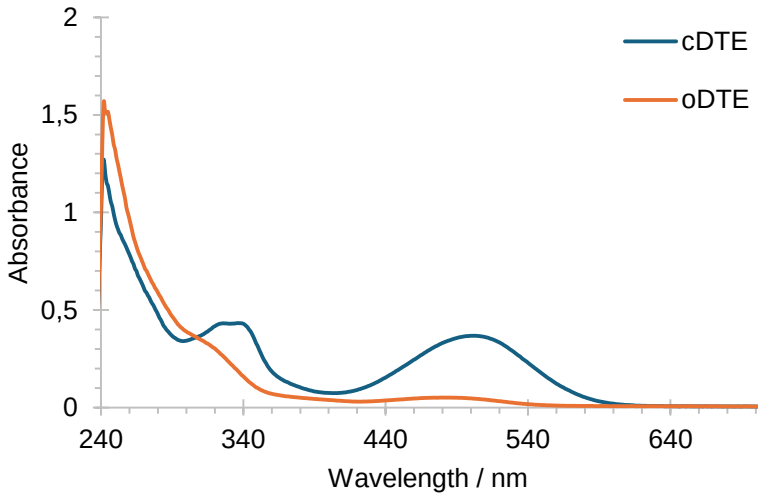

Figure S3. UV absorption spectra of 240 µM **2,2'-PCL** upon irradiation with 311 nm light for 2 min. in dioxane (blue spectra), followed by irradiation with visible light for 10 min. (orange spectra).

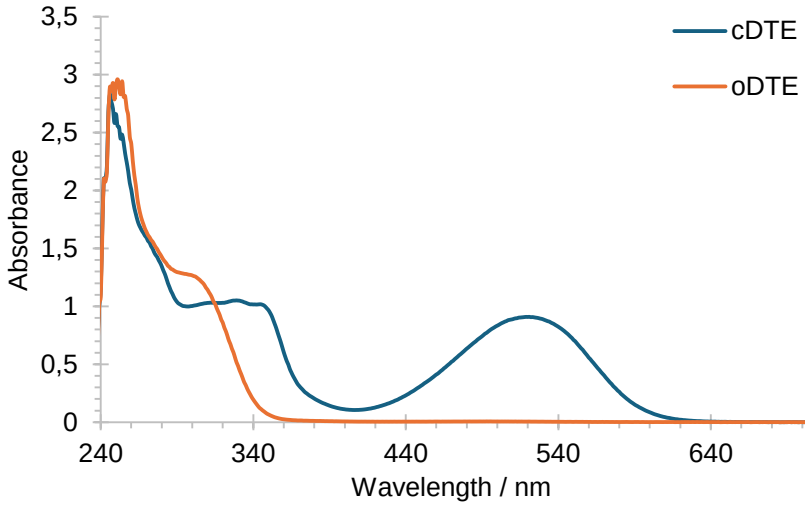

Figure S4. UV absorption spectra of 200 µM **5,5′-diOAc** upon irradiation of 600 µM stock solution in dioxane with 311 nm light for 1.5 min. (blue spectra), followed by irradiation with visible light for 10 min. (orange spectra).

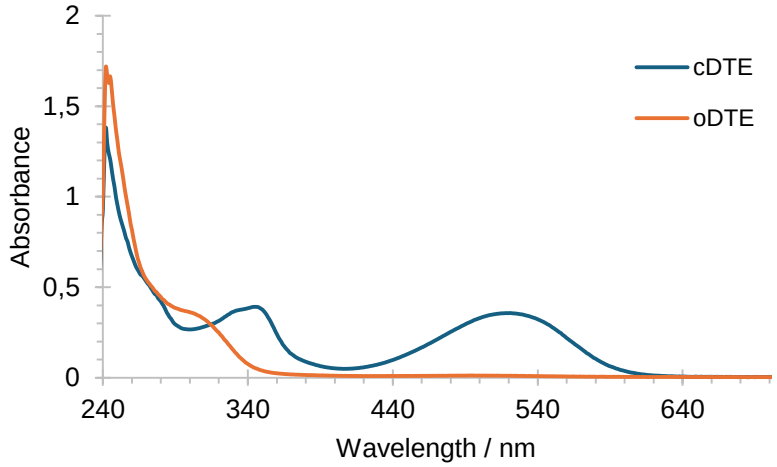

Figure S5. UV absorption spectra of 200 µM **5,5′-PCL** upon irradiation with 311 nm light for 2 min. in dioxane (blue line), followed by irradiation with visible light for 10 min. (orange line).

HPLC Conditions

UV light was passed through a quartz cuvette to irradiate 1.5 mL of stock solutions similar to UV measurement. Subsequently, 500 µL of the exposed solution was added to 1.0 mL of the reference solution in ACN in an HPLC vial. 4,4-dimethyl-2-(5-(4-nitrophenyl)thiophen-2-yl)-4,5-dihydrooxazole was utilized as an internal standard. For the analysis of the **2,2′-diOAc** sample, a 50-

70 % acetonitrile/water gradient run was employed for 0-10 min., followed by an isocratic run of 70% acetonitrile for another 10 min.

The open and closed forms of **5,5′-diOAc** elute simultaneously with this quick HPLC method. However, they were effectively separated using a 25-55% gradient run of acetonitrile/water for 60 minutes, followed by an isocratic run of 55% acetonitrile for another 20 min.

PSS Measurement by HPLC

UV-Vis spectrometry provides the absorption spectra of both open and closed forms of DTE, but it does not offer a quantitative measurement of $_{C}$DTE at photostationary state (PSS). To obtain the quantitative value of $_{C}$DTE at PSS, HPLC has been utilized. Initially, the solution was irradiated with UV light to reach PSS, and HPLC was used to record the results in the presence of an internal reference to determine the relative amount of $_{O}$DTE at PSS. Subsequently, the HPLC sample was irradiated with visible light for 10 minutes to convert all the DTE to the open form, and HPLC was recorded once again. This process helps to measure the amount of oDTE (total DTE) relative to the internal standard. In Figures S2.5 and S2.6, the HPLC spectra of the compounds **2,2′-diOAc** and **5,5′-diOAc** in both open and closed forms are shown.

PSS is calculated through the following equation:

$$PSS = 1 - \frac{\frac{Area_{open,\ after\ UV}}{Area_{std,\ after\ UV}}}{\frac{Area_{open,\ after\ visible}}{Area_{std,\ after\ visible}}}$$

Thus, the calculated amount of cDTE at PSS for **2,2′di-OAc** is 56.4%, and 53.4% for **5,5′di-OAc**.

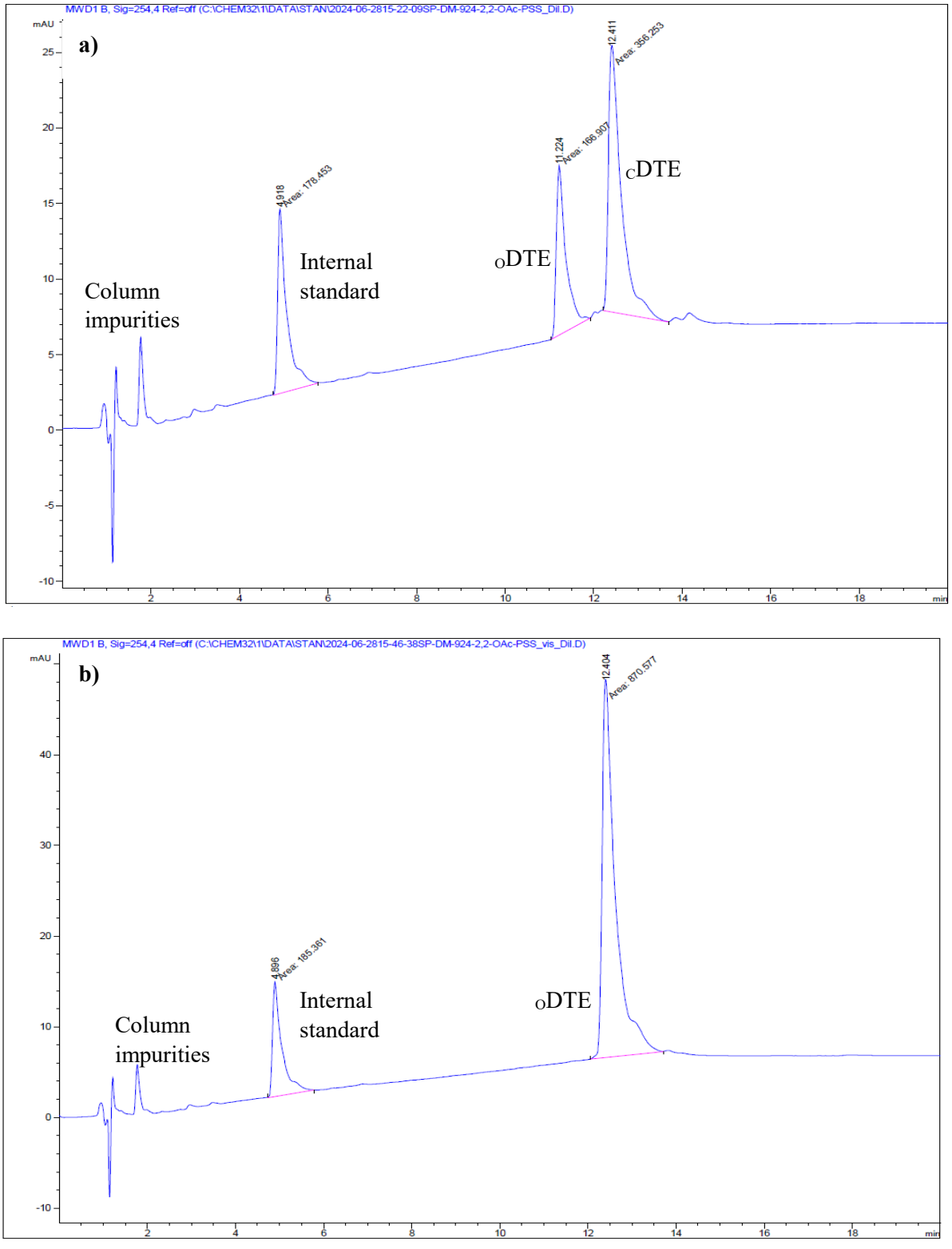

Figure S6. HPLC absorption spectra at 254 nm of **2,2′di-OAc** in the presence of internal standard after a) 2-minute irradiation of 311 nm light, b) 10-minute subsequent irradiation of visible light.

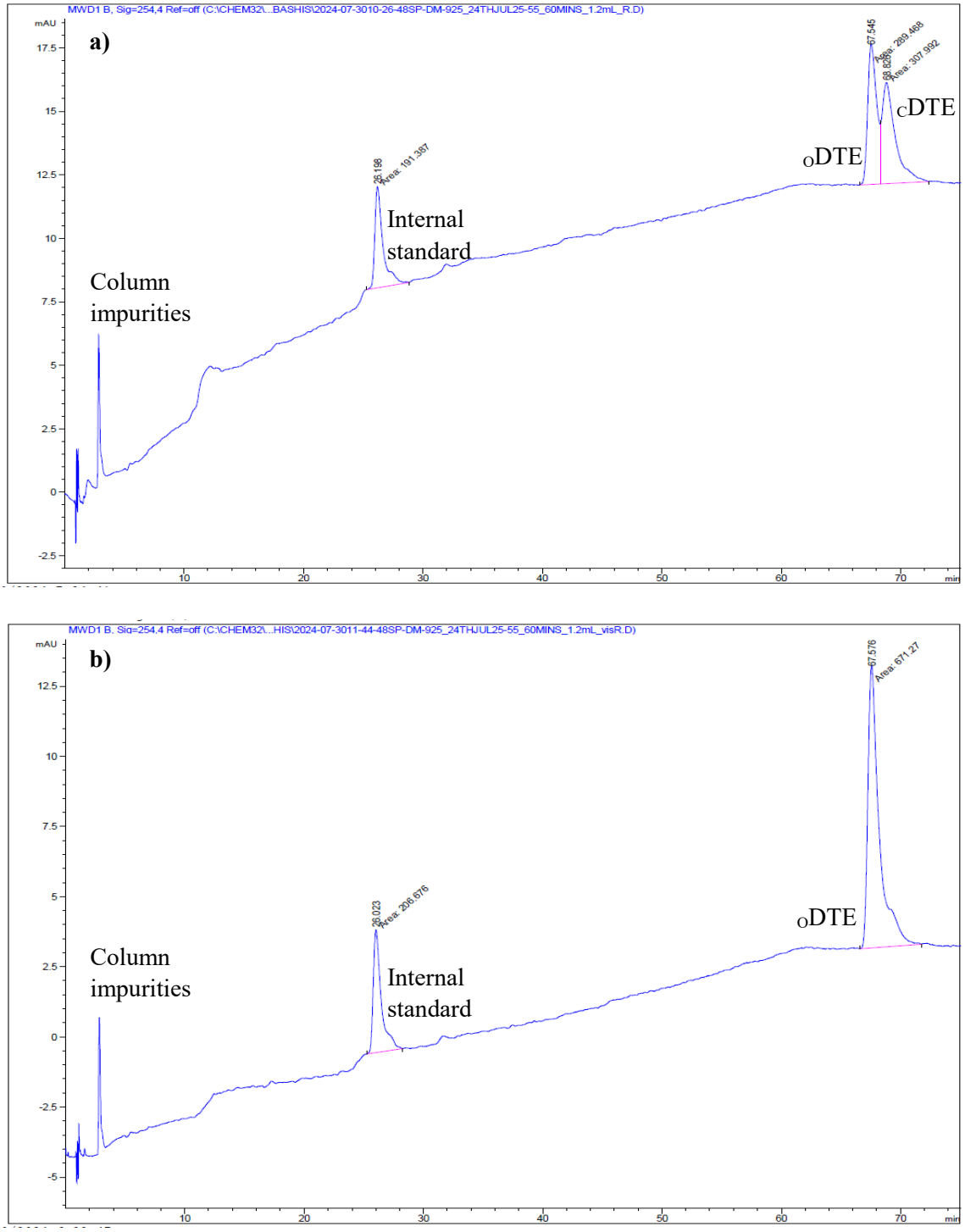

Figure S7. HPLC absorption spectra at 254 nm of **5,5′di-OAc** in the presence of internal standard after a) 1.5-minute irradiation of 311 nm light, b) 10-minute subsequent irradiation of visible light.

PSS Measurements of PCL

Determination of cDTE at PPS for **2,2'-PCL** and **5,5′-PCL** was done by measuring their λ_{max}/ isosbestic point absorption ratios and using the corresponding **di-OAc** ratios as a reference. Based on these, the calculated electrocyclization extent for **2,2'-PCL** is 58% and for **5,5′-PCL** is 71% at PSS.

Computational Details

All the CoGEF simulations were performed using the ORCA computational package[1], employing the XTB2[2] method unless otherwise indicated. The unconstrained equilibrium geometry (Figure S8 and Figure S9) was obtained by optimizing the original cDTE structure from the experimental data. Starting from the equilibrium structure, the distance between 2,2'-positions was increased in increments of 0.05 Å, and then constraint optimization was performed at each step. Calculations were run until a chemical transformation was predicted to occur, as evidenced by the rupture and reorganization of the ring opens or the rupture of one or more covalent bonds. The distance on the 2,2'-positions was elongated from 3.974 Å to 5.324 Å. Likewise, the simulations along the 5,5'-positions were from increasing the distance between the 5,5'-positions incrementally by 0.05 Å, starting from the equilibrium structure. At each increment, a constraint optimization was conducted. The process continued until a chemical transformation was indicated, which was characterized by the opening or reorganization of the molecular ring structure or the breaking of one or more covalent bonds. The distance on the 5,5'-positions was changed from 9.188 Å to 10.788 Å. The maximum force predicted for each ring-opening pathway was calculated from the slope between contiguous points in the energy-displacement curve.

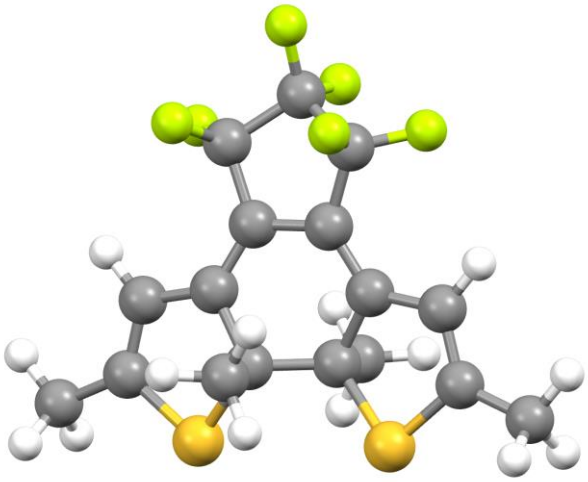

Figure S8. The front view of the optimized structure of the cDTE molecule. The green spheres are F, the yellow spheres are S, the grey spheres are C and the white spheres are H.

The Potential Energy Surface (PES) was obtained to investigate all the possible pathways in the ring-opening process to get a general view of this transformation. From the optimized equilibrium structure, the distance between 2,2'-positions was increased from 3.974 Å to 5.324 Å and decreased from 3.974 to 3.774, with each step as 0.05 Å, and constraint optimizations on each step were performed. Subsequently, all these optimized structures were used separately to conduct constraint optimizations where the distance between 5,5'-positions was slowly increased from 9.188 Å to 13.788 Å and decreased from 9.188 Å to 8.738 Å, with each step as 0.05 Å. To avoid sudden changes in the structure where the computational package would no longer recognize the atoms we pull away as a whole molecule, the optimizations mentioned above were performed one after another, using the geometry of the previously optimized molecule where possible.

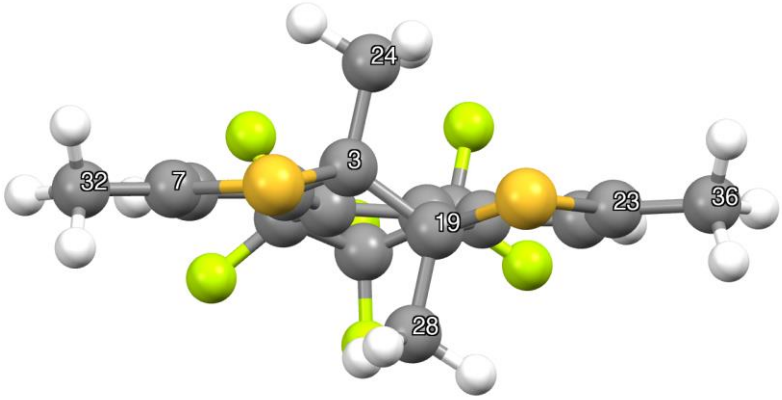

Figure S9 The bottom view of the optimized structure of the cDTE molecule and the labels of different carbon atoms. The green spheres are F atoms, the yellow spheres are S atoms, the grey spheres are C atoms, and the white spheres are H atoms.

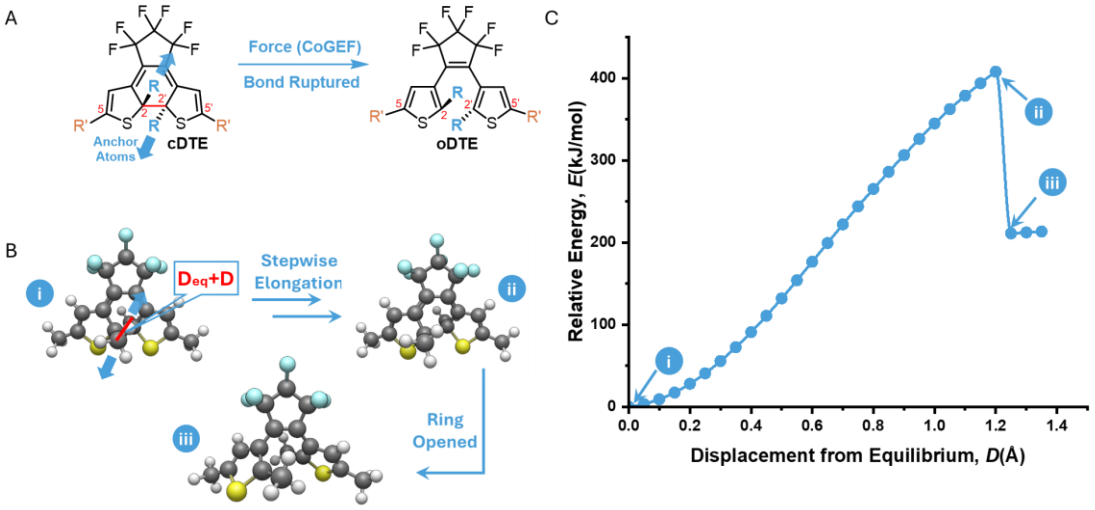

Figure S10. CoGEF method used to simulate the ring-opening process with the stretch on 2,2'-positions of cDTE. (a) Structures of the DTE before and after the ring opened. The groups colored orange designate the anchor points defining the distance constraint. (b) Computed structures at critical points in the CoGEF calculation: (i) the constraint-free equilibrium geometry, (ii) the constrained geometry immediately prior to the ring open, and (iii) the predicted oDTE. (c) Relative energy, E, plotted as a function of displacement from equilibrium, D (Å).

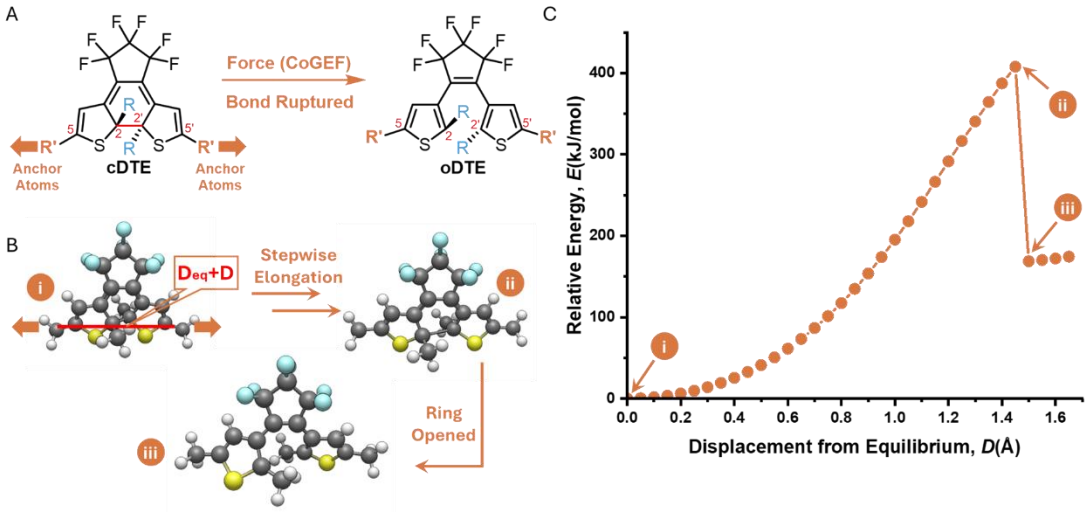

Figure S11. CoGEF method used to simulate the ring-opening process with the stretch on 5,5'-positions of cDTE. (a) Structures of the DTE before and after the ring opened. The groups colored in blue designate the anchor points defining the distance constraint. (b) Computed structures at critical points in the CoGEF calculation: (i) the constraint-free equilibrium geometry, (ii) the constrained geometry immediately prior to the ring opening, and (iii) the predicted oDTE. (c) Relative energy, E, plotted as a function of displacement from equilibrium, D (Å).

Density functional theory (DFT) at the B3LYP/def2-SVP level of theory was used to obtain more accurate relative energy values for the intermediates along the two realistic mechanochemical pathways. The calculated forces required for ring-opening are simply the slope between contiguous points in the energy-displacement curves. The 'spring constant' for each mechanophore is the slope of the linear portion of the force-elongation curve, i.e. the second derivative of its relative energy.

2. Synthesis

2,2'-DTE and 5,5'-DTE photochromic molecules were prepared from commercially available thiophenes following established procedures as summarized in Scheme 1. Different molecular weight polymers containing DTE chromophores were prepared by ROP. Briefly, a typical synthesis of DTE-PCL was performed as follows: a Schlenk flask was charged with freshly distilled ε-caprolactone (CL) (2 g, 0.017 mol), **5,5'-diOH** (7.5 mg, 0.0175 mmol), tin(II) 2-ethylhexanoate (7.1 mg), and anhydrous toluene (10 mL), then degassed by bubbling nitrogen. The reaction was stirred in an oil bath for 36 h at 110 °C. The resulting polymer was diluted with toluene and precipitated into cold methanol three times.

Polymerization of ε-Caprolactone (PCL) with 2,2'-diOH and 5,5'-diOH DTE

ROP polymerization of DTE and ε-caprolactone was carried out in toluene for 24 to 48 hours. The initial molar ratio of the monomer and initiator varies depending on the desired molecular weight, while the catalyst Sn(Oct)2 was kept constant and equal to $[DTE]_0/[Sn(Oct)2]_0=1/3$. Below is a detailed description of one synthesis of the polymer-DTE compound.

A 15 mL Schlenk flask (all glassware was dried overnight in an oven at 160 ^oC.) equipped with a stir bar was charged with freshly distilled ε-caprolactone (CL) (2 g, 0.017 mol) (dried over calcium hydride purified by distillation under reduced pressure and stored in a glovebox under nitrogen), DTE-5,5' (7.5 mg, 0.0175 mmol) and degassed with nitrogen. Then tin(II) 2-ethylhexanoate (7.1 mg) (stirred overnight with anhydrous magnesium sulfate (Aldrich) and distilled) and anhydrous toluene 10 ml (distilled over calcium hydride (CaH_2) and held on a 3A molecular sieve before being used) were added and additionally deoxygenated with nitrogen. The reaction was stirred in an oil bath for 36 h at 110 °C. The reaction was quenched by opening it to the air and putting it into the freezer. The polymer was diluted with toluene, precipitated into cold methanol, and re-dissolved in 1,4-dioxane; the process was repeated three times. The product was filtered off and dried under a vacuum. All obtained compounds were white and had different powdery–fibrous structures (FigureS4), depending on their molecular weight. The yield of compounds varies from 74 – 90 %. ^1H NMR ($CDCl_3$): δ = 1.40 (1H, m), 1.65 (2H, m), 2.31 (1H, t), 4.06 (1H, t)

Poly(ε-caprolactone) synthesis

The $Sn(Oct)_2$-catalyzed polymerization of ε-caprolactone was performed in a 15 mL Schlenk flask (all glassware was dried overnight in an oven at 160 ^oC). A flask was charged with CL (dried over calcium hydride purified by distillation under reduced pressure and stored in a glovebox under nitrogen) monomer, butanol (stirred overnight with anhydrous magnesium sulfate (Aldrich) and distilled), and toluene (distilled over calcium hydride (CaH_2) and held on a 3A molecular sieve before

being used) in a nitrogen atmosphere, the mole ratio of components was $[CL]_0$:$[butanol]_0$:$[Sn(Oct)_2]_0$=350:1:1.5. Then, the reaction flask was kept in an oil bath at 110 ºC for 36 h. The reaction was quenched by opening it to the air and putting it into the freezer. To remove the unreacted monomer and $Sn(Oct)_2$ an excess of methanol was added to the reaction mixture. Polymer powders were isolated by centrifugation, washed twice with additional methanol, and dried in a vacuum oven.

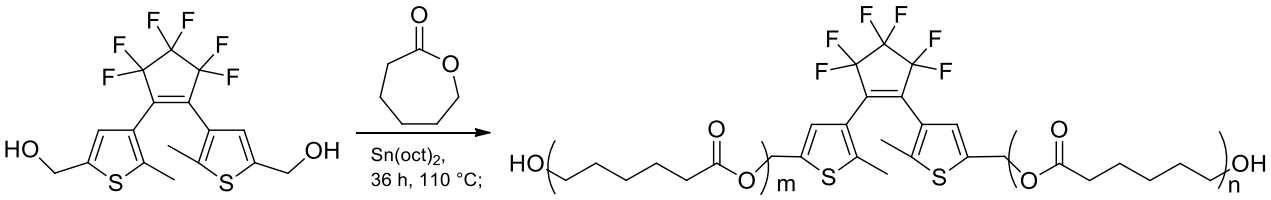

Figure S12. DTE-5,5’ and ε-caprolactone ROP polymerization scheme.

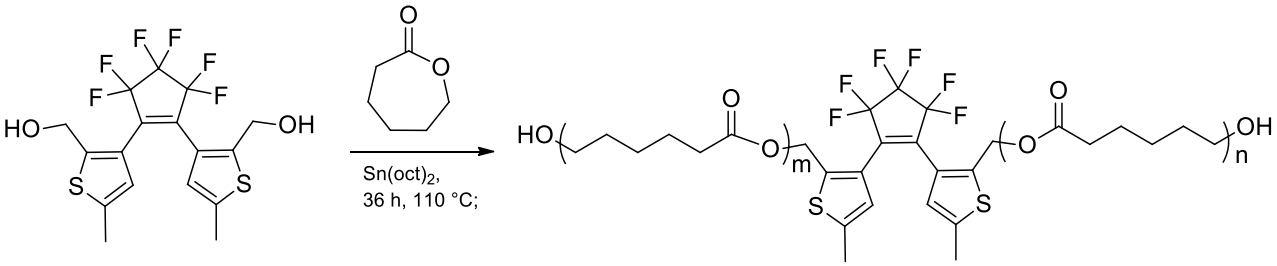

Figure S13. DTE-2,2’ and ε-caprolactone ROP polymerization scheme.

Table S1. Macromolecular results of synthesized 2,2'-PCL and 5,5'-PCL polymers.

No.	Polymer	M_n, kDa	Đ	Yield, %*
1	2,2'-PCL	23.9	1.23	90
2	2,2'-PCL	38.1	1.31	86
3	2,2'-PCL	57.9	1.59	74
4	5,5'-PCL	21.4	1.20	89
5	5,5'-PCL	34.3	1.25	88
6	5,5'-PCL	53.5	1.51	83
7	poly(ε-caprolactone)	38.4	1.30	76

* Calculated from dry yield

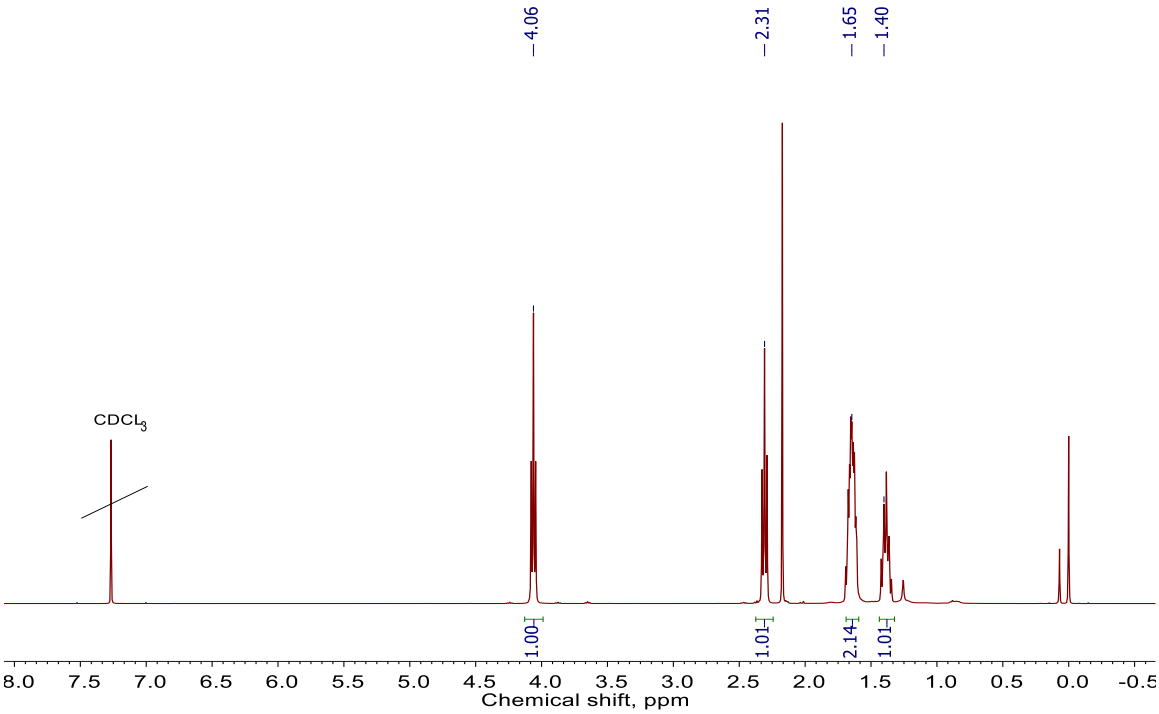

Figure S14. ^{1}H NMR spectrum of DTE-2-(PCL)$_2$ (400 MHz, $CDCl_3$).

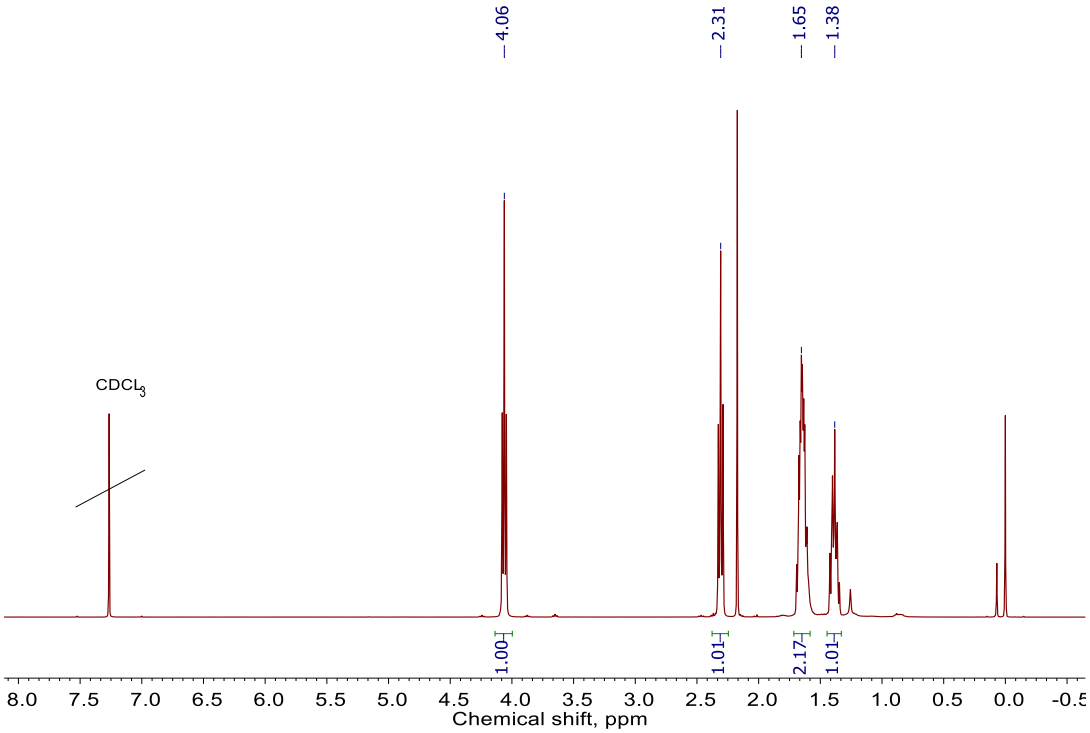

Figure S15. ^{1}H NMR spectrum of DTE-5-(PCL)$_2$ (400 MHz, $CDCl_3$).

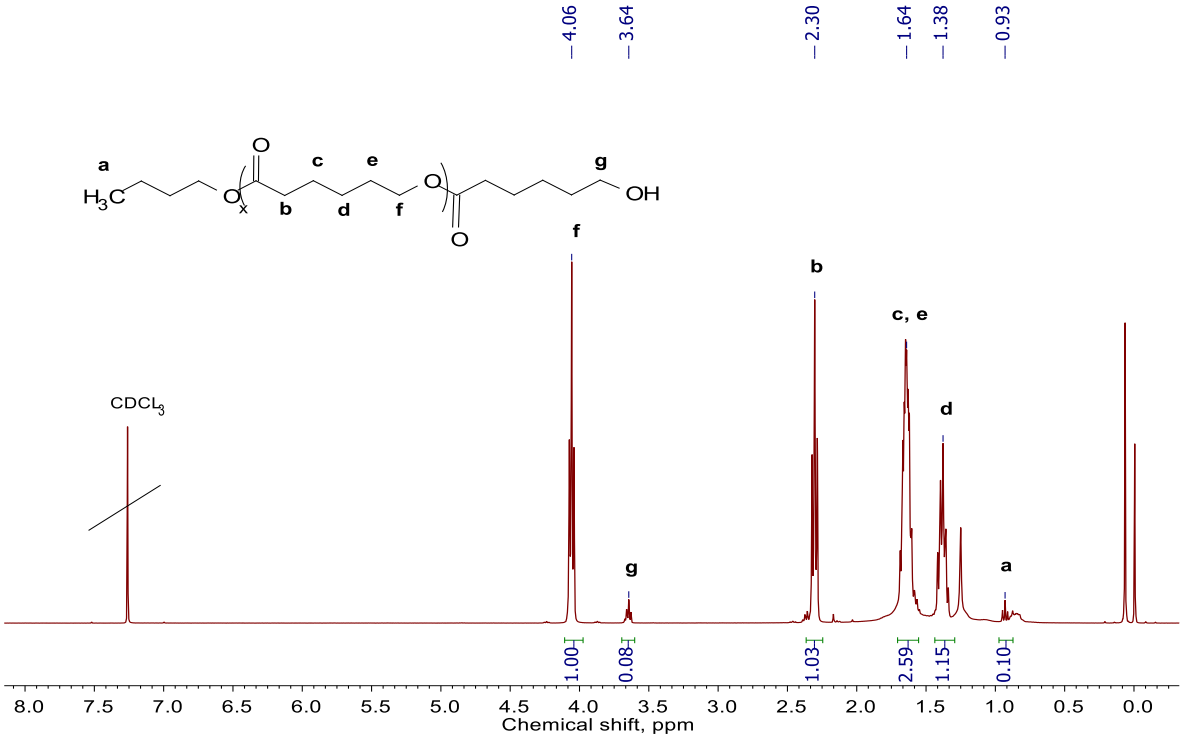

Figure S16. ^{1}H NMR spectrum of poly(ε-caprolactone) (400 MHz, $CDCl_3$).

Synthesis procedure of 2,2′-diOAc

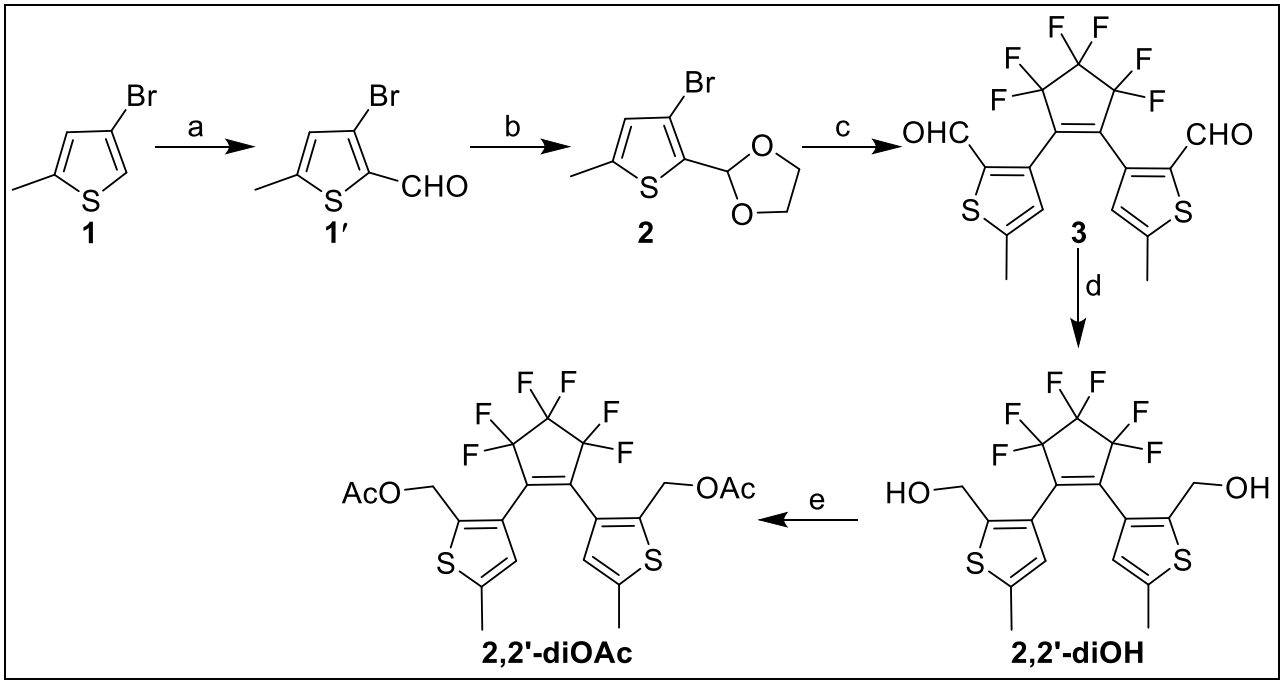

Scheme S1 Synthetic route of 2,2′-diOAc.

a) LDA, DMF, THF, -78 °C-rt (90%); b) Glycol, pTSA, toluene, reflux (92%); c) nBuLi, C_5F_8, -78 °C, HCl (50%); d) $NaBH_4$, MeOH, 0 ° C (86%); e) Ac_2O, DMAP, Et_3N, 0 ° C- rt (75%).

Synthesis of 3-Bromo-5-methyl-2-thiophenecarboxaldehyde (1′)[3]

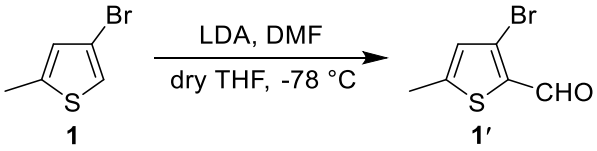

5 grams of commercially available 4-bromo-2-methylthiophene 1 (28.2 mmol, 1.0 eq.) was dissolved in 25 mL of dry THF in an oven-dried 100 mL 2-neck round bottom flask. The reaction mixture was placed at -78 °C under a nitrogen atmosphere, and 31mL of 1.0 M LDA in THF (1.1eq.) was added dropwise to the reaction mixture through a syringe and stirred for 1 h. Then, 2.8 mL of *N, N*-dimethylformamide (36.7 mmol, 1.3 equiv.) in 10 mL dry THF was added to the mixture. The resulting solution was stirred for another hour and gradually warmed to room temperature. The reaction mixture was then quenched with ice-cold water, and after evaporating the excess THF, it was extracted with ethyl acetate. The combined organic layer was dried with anhydrous sodium sulfate and evaporated using a rotary evaporator. The crude product was purified by silica gel flash chromatography using a Hexane/Ethyl acetate (95:5) eluent to obtain 5.2 grams of pure pale-yellow solid 1′ (25.5 mmol, 90%).

^{1}H NMR (400 MHz, $CDCl_3$) δ 9.86 (s, 1H), 6.84 (s, 1H), 2.55 (s, 3H). ^{13}C NMR (101 MHz, $CDCl_3$) δ 182.72, 151.20, 135.03, 130.62, 120.51, 16.52.

Synthesis of 2-(3-Bromo-5-methyl-2-thienyl)-1,3-dioxolane (2)[5]

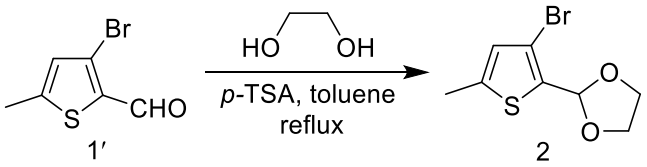

3-bromo-5-methylthiophene-2-carbaldehyde (1′) (2.5 g, 12.2 mmol, 1.0 equiv.), p-toluenesulfonic acid monohydrate (116 mg, 0.6 mmol, 0.05 equiv.), and ethylene glycol (10.0 ml, 183 mmol, 15.0 equiv.) were combined in a 100 ml round bottom flask with 50 ml of toluene. The mixture was refluxed using a Dean-Stark trap for 2 hours. Upon completion, the reaction was diluted with ethyl acetate and washed with water to remove excess ethylene glycol. The combined organic phase was dried with anhydrous sodium sulfate and concentrated under reduced pressure. The crude product was purified by silica gel flash column chromatography using 5% ethyl acetate/hexane as the eluent, resulting in the isolation of pure 2.8 gm of desired compound 2 as a yellow oil (11.2 mmol, 92%).
^{1}H NMR (400 MHz, $CDCl_3$) δ 6.65 – 6.60 (m, 1H), 6.06 (s, 1H), 4.18 – 4.11 (m, 2H), 4.03 – 3.96 (m, 2H), 2.44 (s, 3H). ^{13}C NMR (101 MHz, $CDCl_3$) δ 141.24, 133.27, 128.33, 109.54, 99.73, 65.47, 15.63. HRMS (ESI) m/z calcd for $C_8H_{10}Br^{79}O_2S$ ($[M+H]^+$): 248.9580, found 248.9575. $C_8H_{10}Br^{81}O_2S$ ($[M+H]^+$): 250.9559, found 250.9560.

Synthesis of 3,3'- (perfluorocyclopent-1-ene-1,2-diyl)bis (5-methylthiophene-2-carbaldehyde) (3)[4]

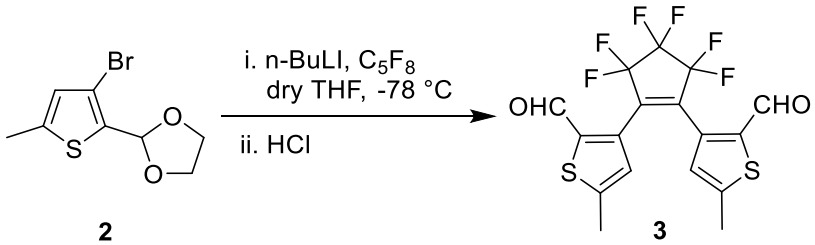

2.0 grams of compound **2** (8.0 mmol, 2.2 equivalents) was dissolved in 15 mL of dry THF in an oven-dried 50 mL 2-neck round bottom flask. The reaction mixture was placed in a -78°C cooling bath, and 4.4 mL *n*-BuLi (2.0 mmol in hexane, 2.4 eq.) was added dropwise. After 1 h of stirring, C_5F_8 (0.490 mL, 3.6 mmol, 1.0 eq.), dissolved in 5 mL of THF, was added to the mixture and stirred for 30 mins at the same temperature, then gradually increased to room temperature. The mixture was hydrolyzed with the addition of 5 mL of concentrated HCl after another hour of stirring. Excess THF was removed, and the reaction mixture was extracted with ethyl acetate/water. The combined organic

phase was dried with anhydrous sodium sulfate, followed by concentration under reduced pressure. The crude product was purified by silica gel flash column chromatography using 5% ethyl acetate/hexane as the eluent, which yielded 770 mg of pure compound 3 as a white solid (2 mmol, 50 %). ^{1}H NMR (400 MHz, $CDCl_3$) δ 9.44 (s, 2H), 6.92 (s, 2H), 2.56 (d, *J* = 1.0 Hz, 6H). ^{13}C NMR (101 MHz, $CDCl_3$) δ 180.12, 152.34, 139.74, 132.62, 127.97, 16.34. ^{19}F NMR (377 MHz, $CDCl_3$) δ -110.79 (t, *J* = 5.0 Hz), -131.47 (p, *J* = 4.8 Hz). HRMS (ESI) m/z calcd for $C_{17}H_{10}F_6NaO_2S_2$ ($[M+Na]^+$): 446.9919, found 446.9920.

Synthesis of ((perfluorocyclopent-1-ene-1,2-diyl)bis (5-methylthiophene-3,2-diyl)) dimethanol (2,2′-diOH)[5]

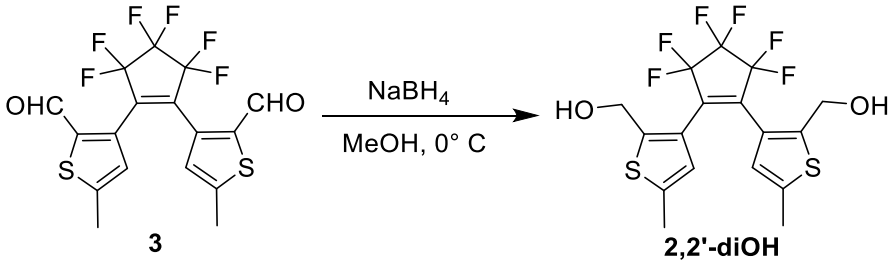

500 mg of compound 3 (1.2 mmol, 1.0 eq.) was dissolved in 10 ml of MeOH and cooled to 0 °C. $NaBH_4$ (275 mg, 7.2 mmol, 6 eq.) was then added in portions to the mixture and stirred for 1 h at the same temperature. After completion, the reaction was quenched by adding aqueous sodium bicarbonate solution, followed by extraction with ethyl acetate. The combined organic layers were dried with anhydrous Na_2SO_4, and the solvent was evaporated using a rotavapor. The crude mixture was purified by silica gel flash column chromatography using Hexane/Ethyl acetate (60:40) as an eluent, resulting in the isolation of pure 2,2′-diOH as a white solid (435 mg, 1.0 mmol, 86% yield).
^{1}H NMR (400 MHz, $CDCl_3$) δ 6.75 (q, *J* = 1.2 Hz, 2H), 4.16 (d, *J* = 5.9 Hz, 4H), 2.47 (s, 6H), 1.83 (t, *J* = 6.2 Hz, 2H). ^{13}C NMR (101 MHz, $CDCl_3$) δ 144.05, 141.28, 125.16, 123.82, 58.69, 15.47. ^{19}F NMR (377 MHz, $CDCl_3$) δ -110.48 (t, *J* = 5.4 Hz), -131.90 (p, *J* = 5.4 Hz). HRMS (ESI) m/z calcd for $C_{17}H_{13}F_6O_2S_2$ ($[M-H]^-$): 427.0266, found 427.0266.

Synthesis of ((perfluorocyclopent-1-ene-1,2-diyl)bis(5-methylthiophene-3,2-diyl)) bis(methylene) (2,2′-diOAc)[6]

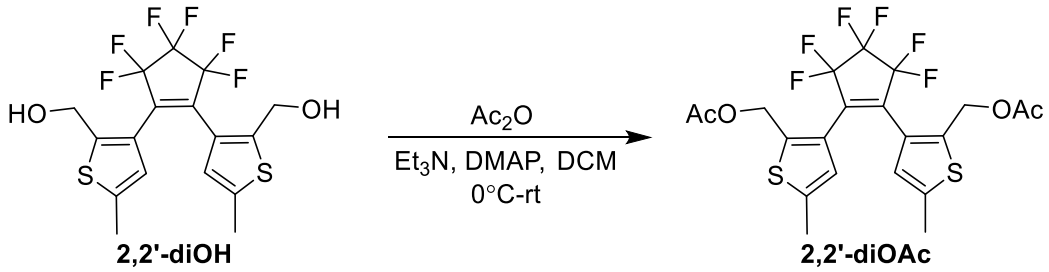

215 mg of 2,2′-diOH (0.5 mmol, 1.0 equivalent) was dissolved in 6 mL of dry DCM. Then, 210 µL of triethylamine (1.5 mmol, 3.0 equivalents) and 110 µL of acetic anhydride (1.2 mmol, 2.4 equivalents) were added to the solution. The reaction mixture was cooled to 0 °C in an ice water bath. After that, 6 mg of DMAP (0.05 mmol, 0.1 equivalent) was added, and the temperature was gradually raised to room temperature. The reaction was stirred until completion, and TLC monitored its progress. After completion, the reaction was stopped by adding a saturated aqueous solution of NH_4Cl. The mixture was then extracted with DCM. The combined organic layers were dried over anhydrous Na_2SO4 and concentrated using a rotary evaporator. The crude product was purified by silica gel flash column chromatography, using ethyl acetate/hexane as an eluent, to obtain pure 2,2′-diOAc as a white solid in 75% yield.

^{1}H NMR (400 MHz, $CDCl_3$) δ 6.79 (d, *J* = 1.2 Hz, 2H), 4.56 (s, 4H), 2.47 (d, *J* = 1.1 Hz, 6H), 1.96 (s, 6H). ^{13}C NMR (101 MHz, $CDCl_3$) δ 170.36, 141.84, 137.47, 125.85, 125.27, 59.12, 20.72, 15.36. ^{19}F NMR (377 MHz, $CDCl_3$) δ -110.75 (t, *J* = 5.3 Hz), -131.84 (p, *J* = 5.4 Hz). HRMS (ESI) m/z calcd for $C_{21}H_{18}F_6O_4S_2Na$ ($[M+Na]^+$): 535.0443, found 535.0445.

Synthetic procedure of 5,5′-diOAc.

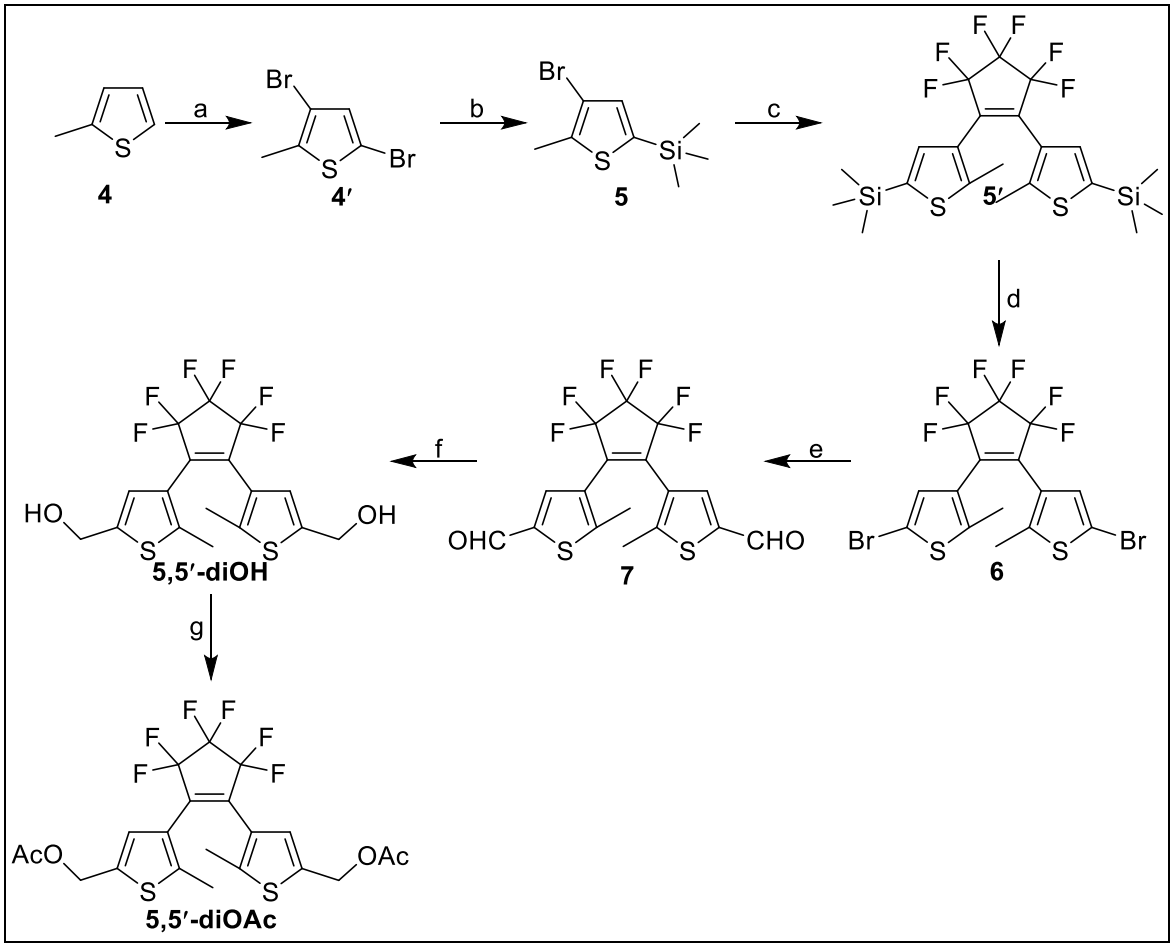

Scheme S2. Synthetic route of **5,5′-diOAc.**

a) NBS, AcOH, rt (92%); b) n-BuLi, THF, -78 °C, TMSCl (90%); c) n-BuLi, THF, -78 °C, C_5F_8(65%); d) NBS, THF (92%); e) n-BuLi, THF, -78 °C - rt, DMF (66%); f) $NaBH_4$, MeOH, 0 °C (80%); g) Ac_2O, DMAP, Et_3N, °C- rt (75%).

Di-bromo DTE (**6**) has been synthesized according to our previously published procedure with an overall yield of 50%.[6] The detailed synthetic procedure discusses starting from compound 7, with the total scheme to synthesize 5,5′-diOAc in Figure S3.5

Synthesis of 4,4'-(perfluorocyclopent-1-ene-1,2-diyl) bis (5-methylthiophene-2-carbaldehyde) (7)[8]

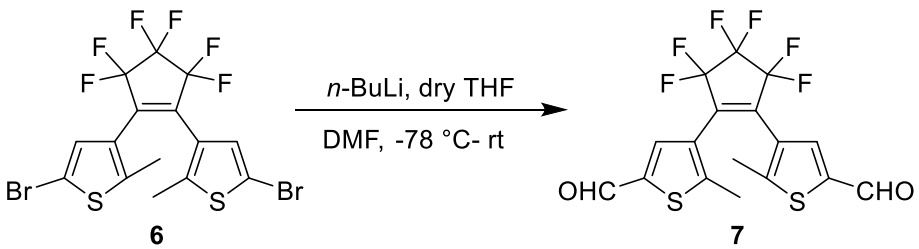

2.1 grams of di-Br DTE (6) (4 mmol, 1.0 equivalent) were dissolved in 20 mL of dry THF in an oven-dried 100 mL 2-neck round bottom flask. The reaction mixture was placed in a -78°C cooling bath, and 4.4 mL of *n*-BuLi (2.0 mmol in hexane, 1.1 equivalent) was added dropwise. After stirring for 1 hour at the same temperature, 1.3 mL dry DMF (16 mmol, 2 equivalents) was added to the mixture and stirred for 30 minutes at the same temperature. Then the reaction was allowed to warm to room temperature and was stirred for another 2 h. The reaction was quenched with saturated NH_4Cl solution, and the excess THF was removed by a rotavapor followed by extraction with ethyl acetate. The combined organic phase was dried with anhydrous Na_2SO_4 and evaporated. The crude product was purified by flash column chromatography using ethyl acetate/hexane (1:10) as eluent, yielding 1.1 grams of pale-yellow solid of 7 (2.6 mmol, 66% yield).

^{1}H NMR (400 MHz, $CDCl_3$) δ 9.85 (s, 2H), 7.73 (s, 2H), 2.03 (s, 6H). ^{13}C NMR (101 MHz, $CDCl_3$) δ 182.04, 151.75, 142.37, 135.79, 126.02, 15.56. ^{19}F NMR (377 MHz, $CDCl_3$) δ -110.32 (t, J = 5.1 Hz), -131.81 (p, J = 5.3 Hz). HRMS (ESI) m/z calcd for $C_{17}H_{10}F_6NaO_2S_2$ ($[M+Na]^+$): 446.9919, found 446.9920.

Synthesis of ((perfluorocyclopent-1-ene-1,2-diyl) bis (5-methylthiophene-4,2-diyl)) dimethanol (5,5′ -diOH)[5]

The reduction of **7** to 5,5′-diOH was carried out using the previously established procedure to reduce **3** with $NaBH_4$, resulting in an 80% yield.

((perfluorocyclopent-1-ene-1,2-diyl) bis (5-methylthiophene-4,2-diyl)) dimethanol (5,5′ -diOH)

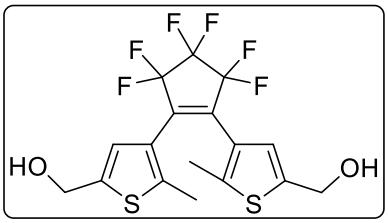

while powder, 80 % yield, ^{1}H NMR (400 MHz, $CDCl_3$) δ 6.94 (s, 1H), 4.75 (s, 2H), 1.92 (s, 1H), 1.89 (s, 3H). ^{13}C NMR (101 MHz, $CDCl_3$) δ 142.32, 142.28, 125.06, 124.60, 60.05, 14.64. ^{19}F NMR (377 MHz, $CDCl_3$) δ -110.12 (t, J = 5.5 Hz), -131.92 (p, J = 5.5 Hz). HRMS (ESI) m/z calcd for $C_{17}H_{13}F_6O_2S_2$ ($[M-H]^-$): 427.0266, found 427.0268.

Synthesis of ((perfluorocyclopent-1-ene-1,2-diyl)bis(5-methylthiophene-4,2-diyl))bis(methylene) diacetate (5,5′-diOAc), white powder, 75% yield

The acetyl protection of 5,5′-diOH was performed using the same procedure as for 2,2′-diOH to yield 2,2′-diOAc with a 75% reaction yield.

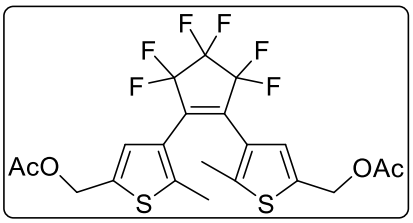

^{1}H NMR (400 MHz, $CDCl_3$) δ 7.01 (s, 2H), 5.14 (s, 4H), 2.08 (s, 6H), 1.87 (s, 6H). ^{13}C NMR (101 MHz, $CDCl_3$) δ 170.73, 143.42, 136.47, 127.87, 124.52, 60.40, 21.00, 14.48. ^{19}F NMR (377 MHz, $CDCl_3$) δ -110.23 (t, J = 5.4 Hz), -131.96 (p, J = 5.4 Hz). HRMS (ESI) m/z calcd for $C_{21}H_{18}F_6O_4S_2Na$ ($[M+Na]^+$): 535.0443, found 535.0446.

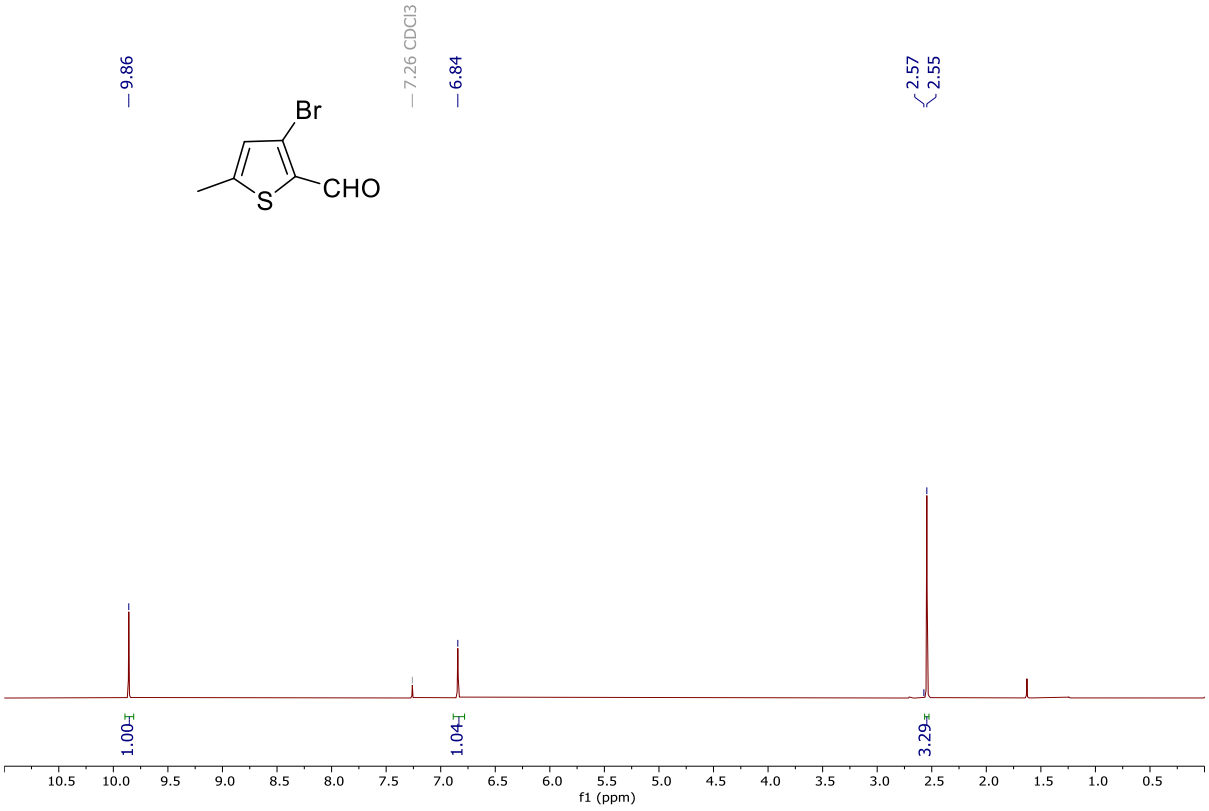

Figure S17. ^{1}H NMR spectrum (400 MHz, $CDCl_3$) of **1′**.

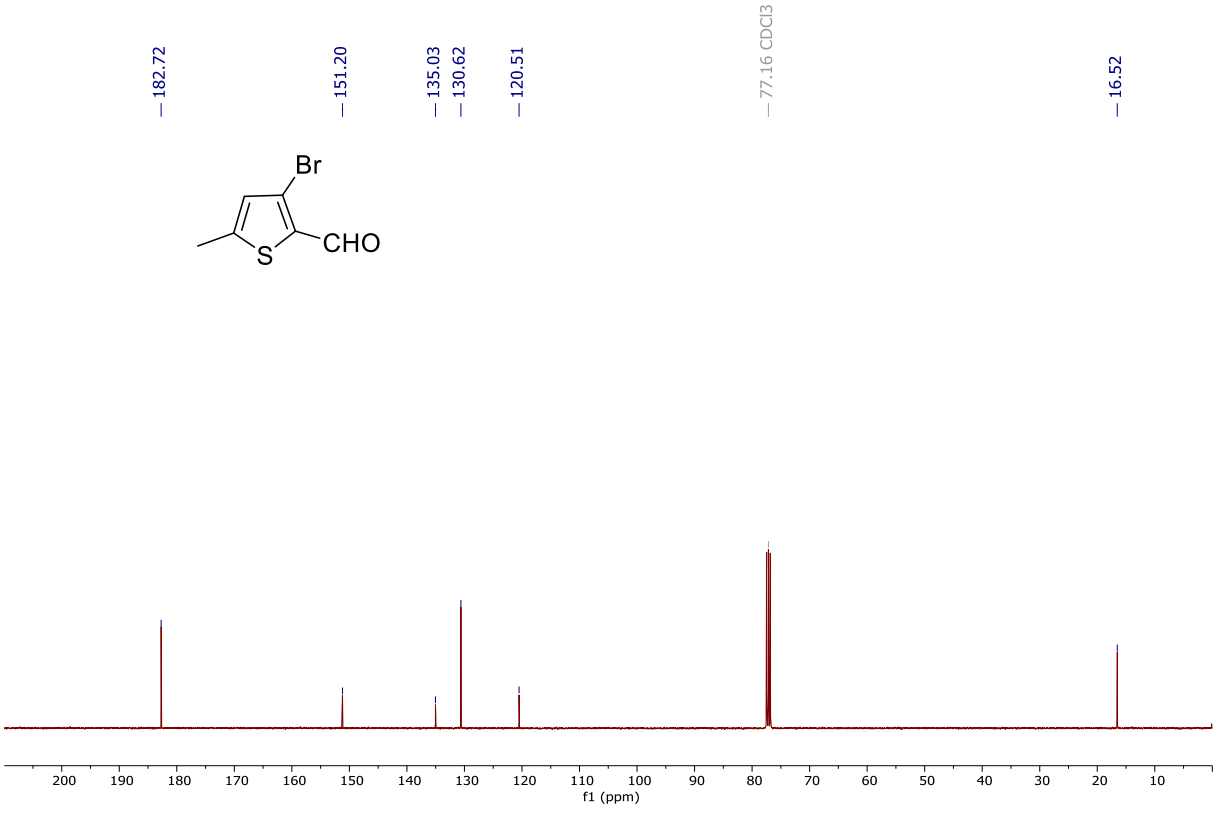

Figure S18. ^{13}C NMR spectrum (100 MHz, $CDCl_3$) of **1′**.

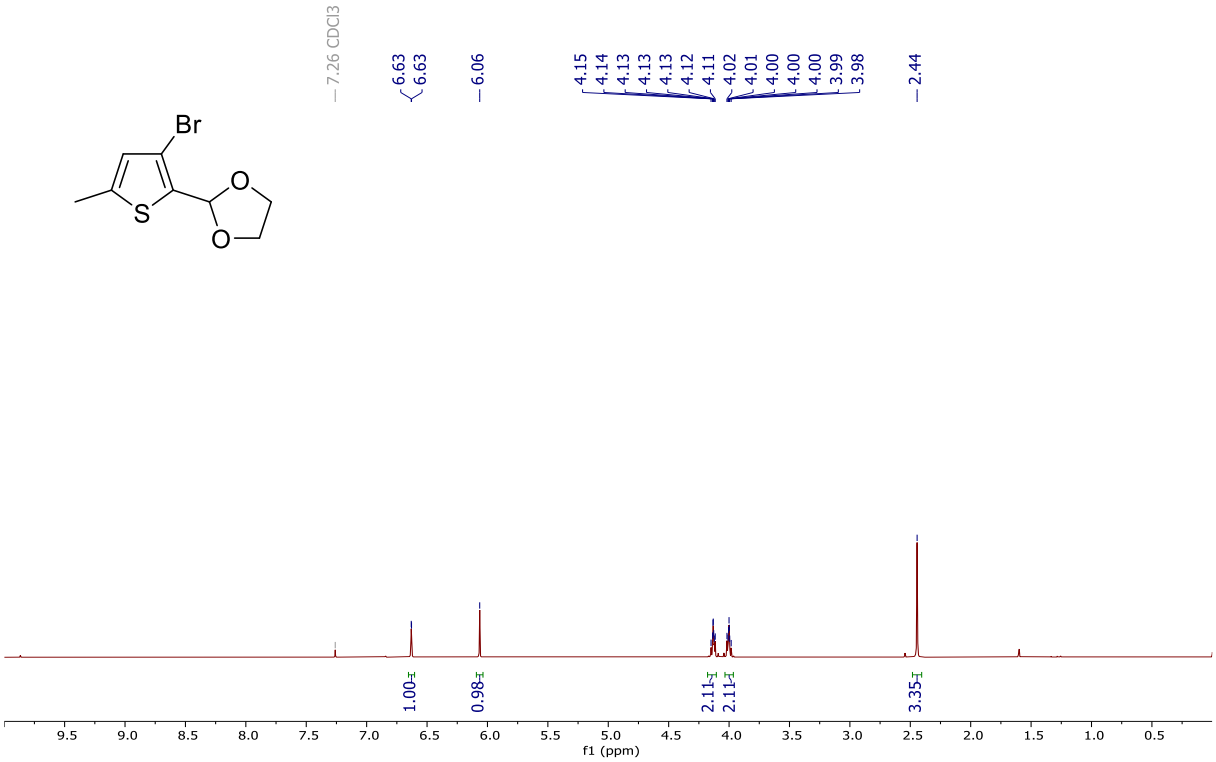

Figure S19. ^{1}H NMR spectrum (400 MHz, $CDCl_3$) of **2**.

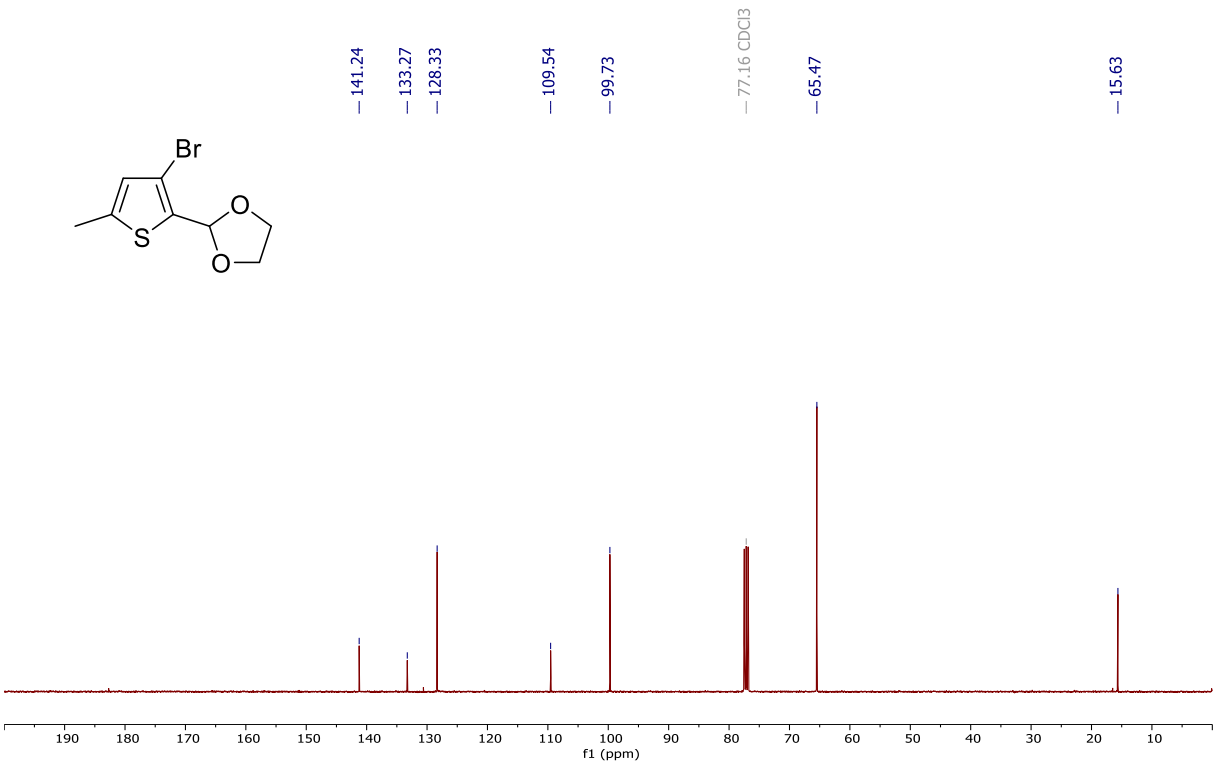

Figure S20. ^{13}C NMR spectrum (100 MHz, $CDCl_3$) of **2**.

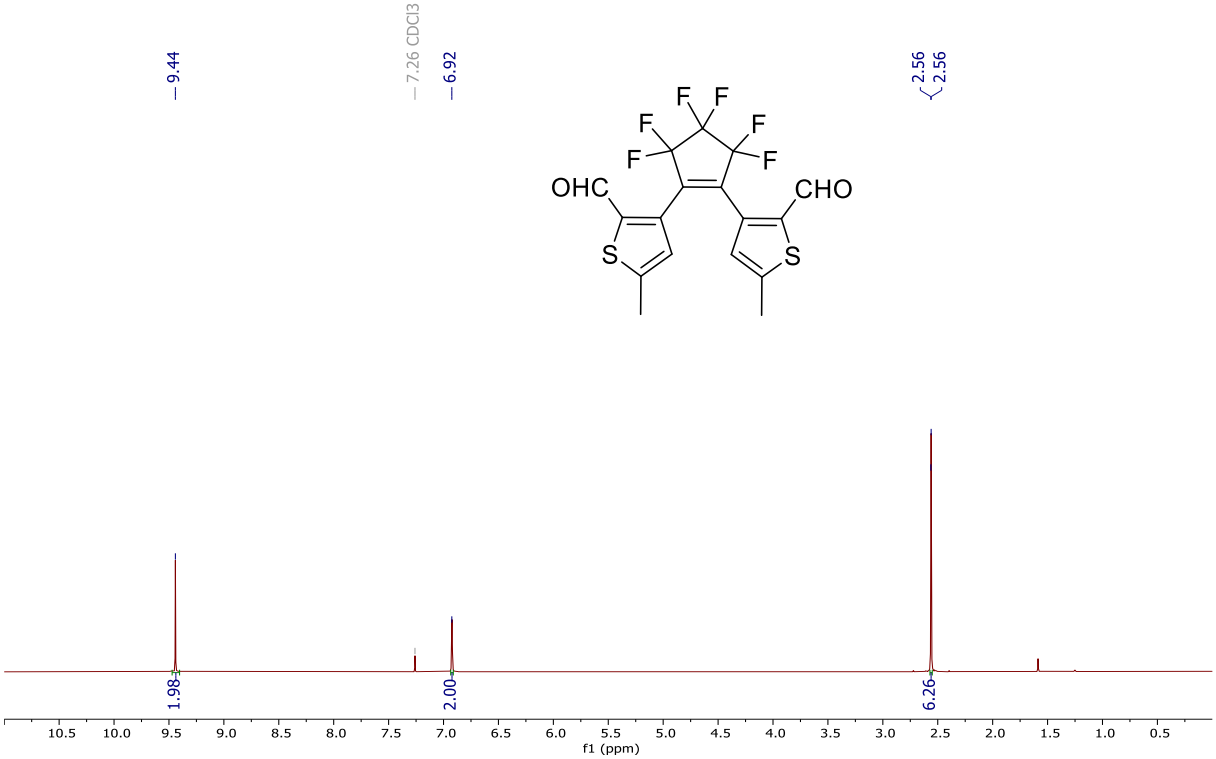

Figure S21. ^{1}H NMR spectrum (400 MHz, $CDCl_3$) of **3**.

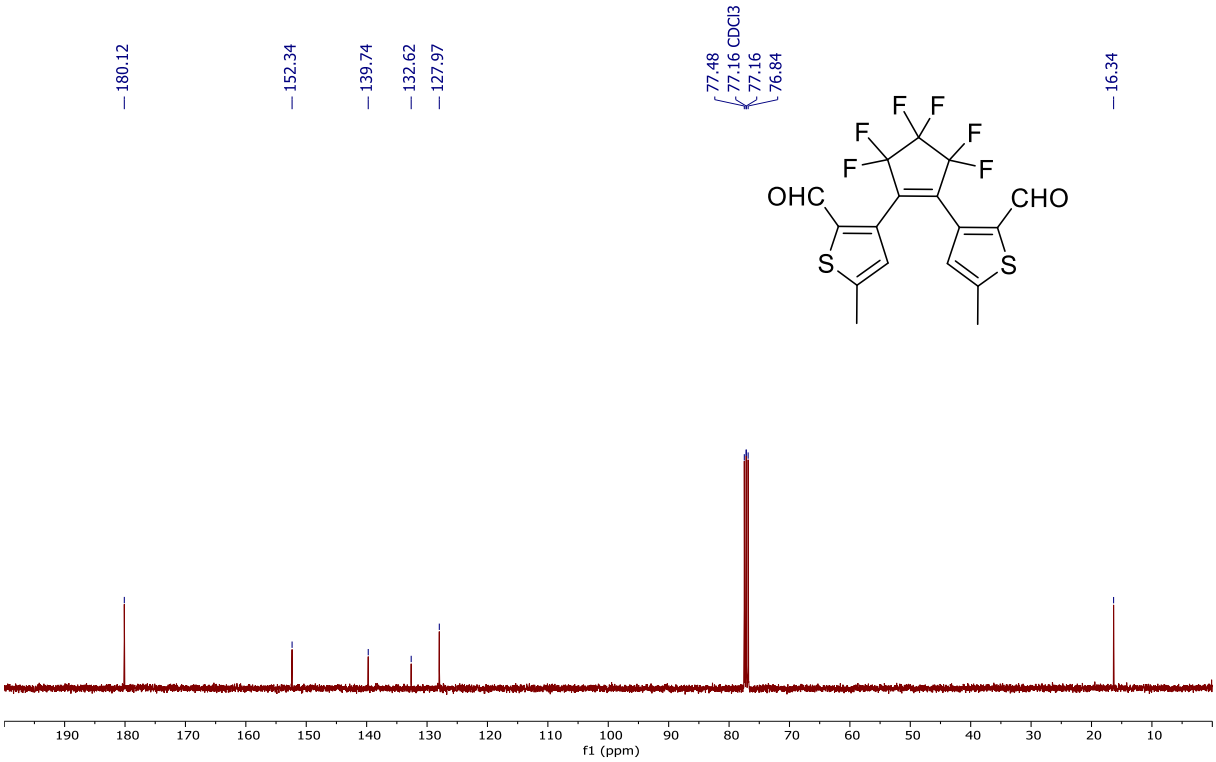

Figure S22. ^{13}C NMR spectrum (100 MHz, $CDCl_3$) of **3**.

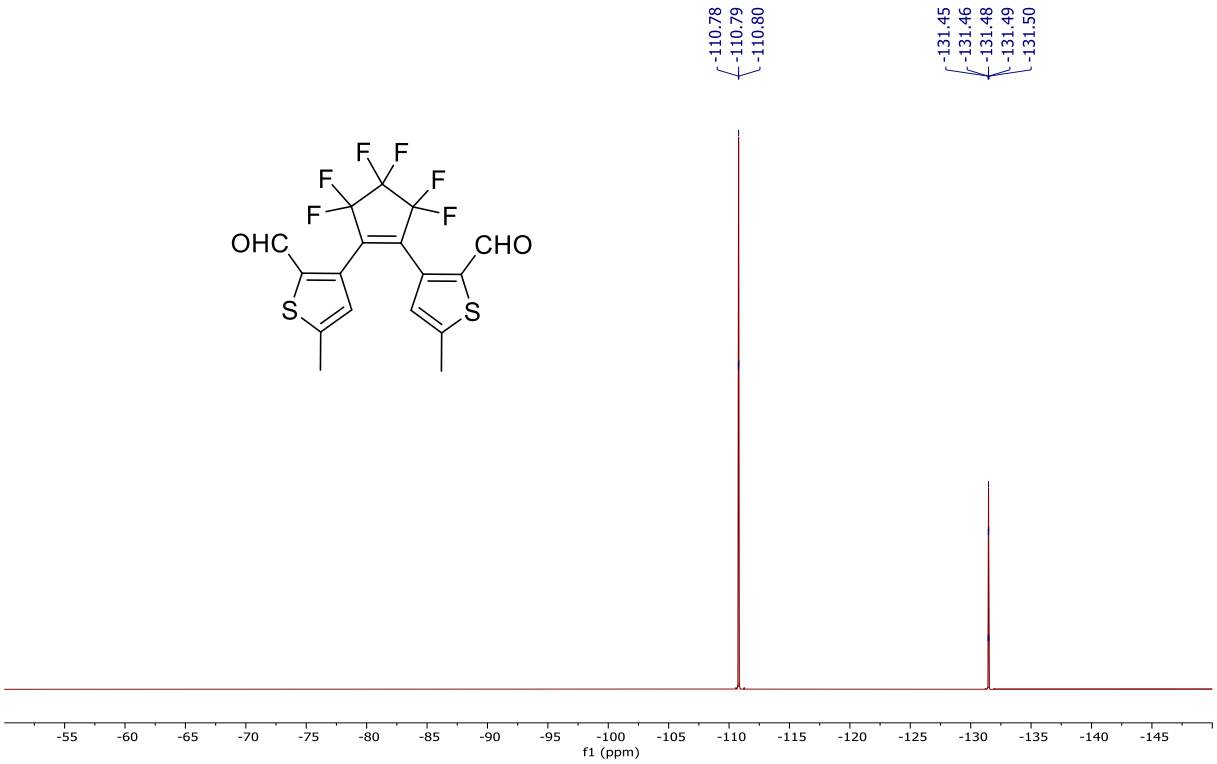

Figure S23. ^{19}F NMR spectrum (377 MHz, $CDCl_3$) of **3**.

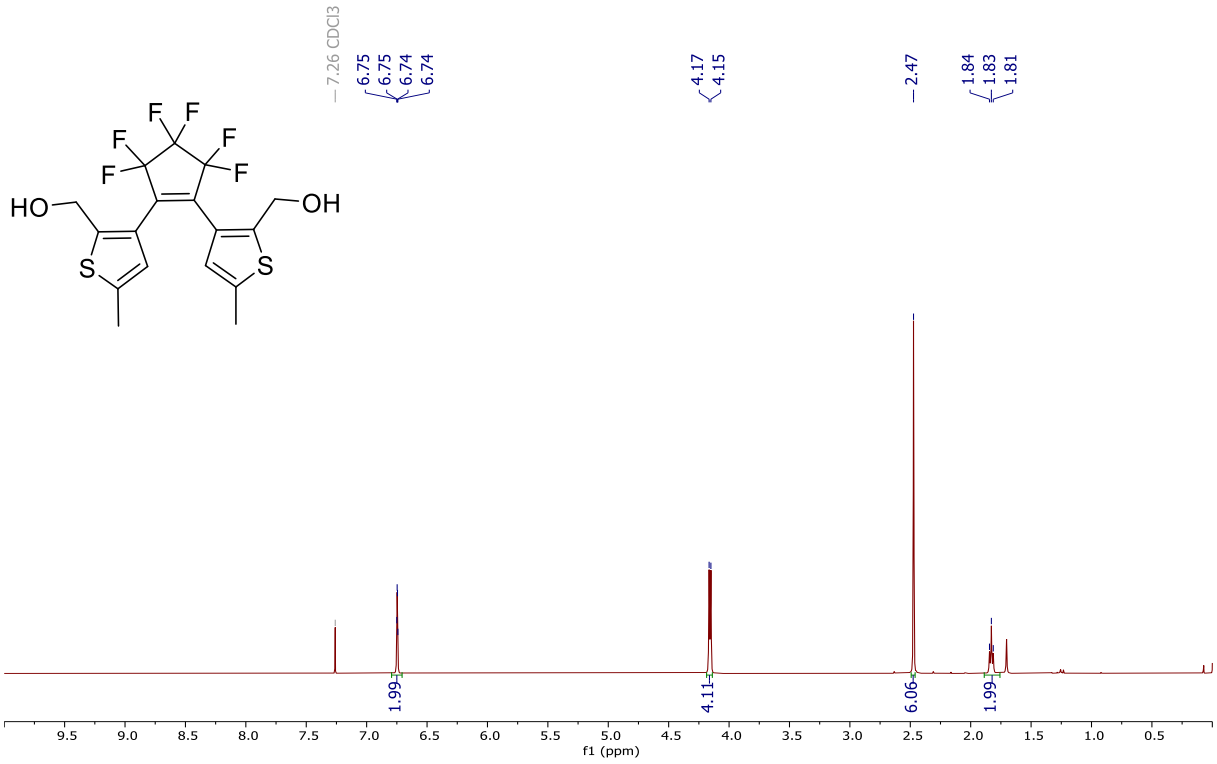

Figure S24. ^{1}H NMR spectrum (400 MHz, $CDCl_3$) of **2,2′-diOH**.

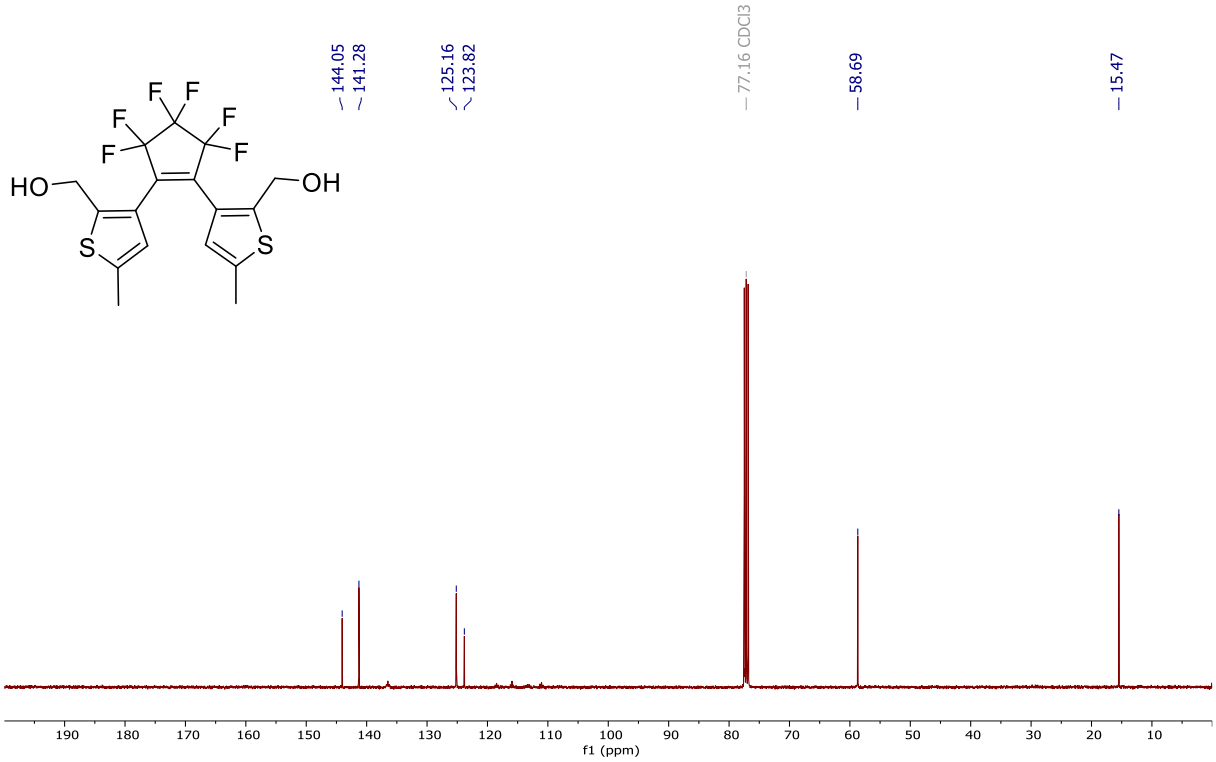

Figure S25. ^{13}C NMR spectrum (100 MHz, $CDCl_3$) of **2,2′-diOH**.

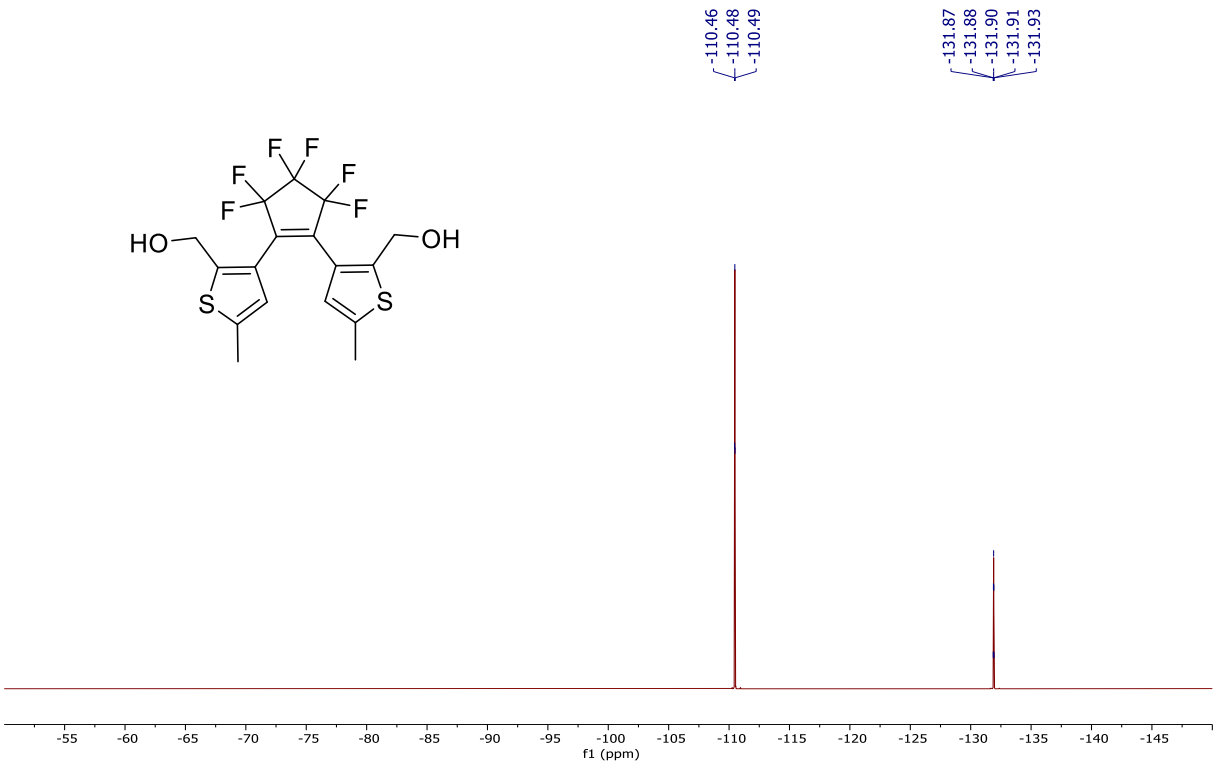

Figure S26. ^{19}F NMR spectrum (377 MHz, $CDCl_3$) of **2,2′-diOH**.

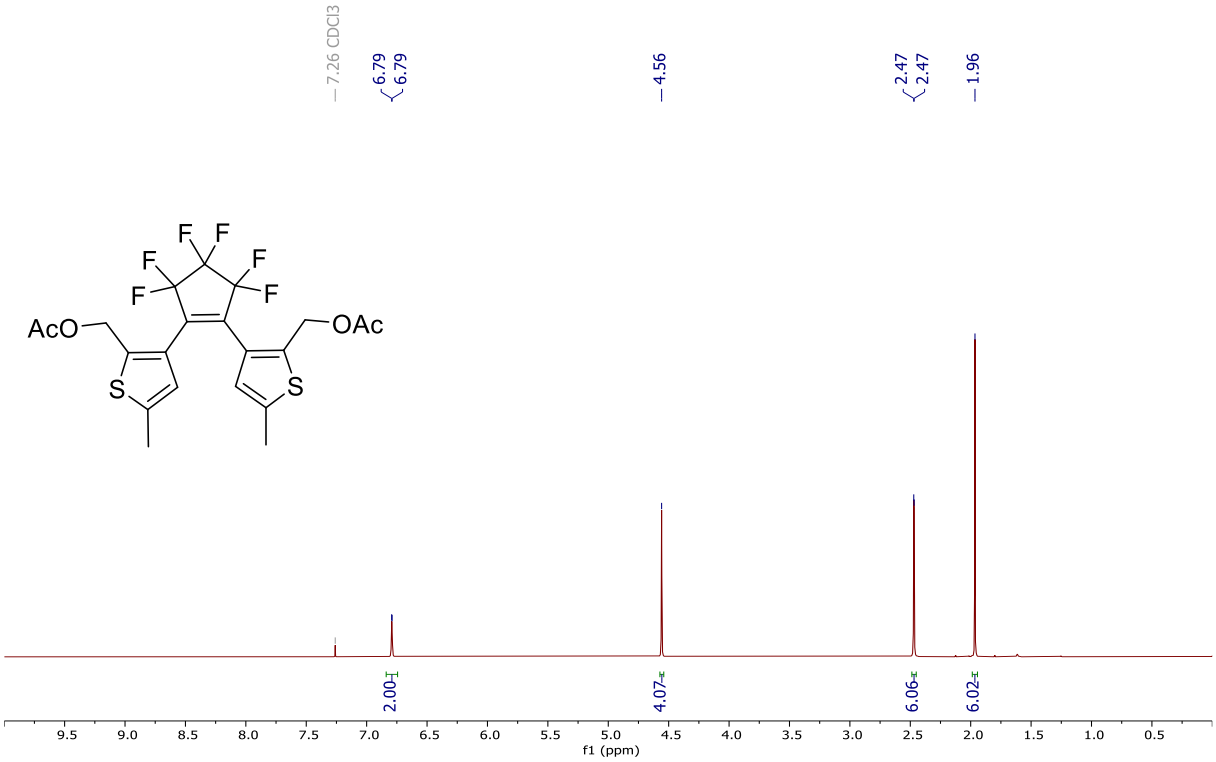

Figure S27. ^{1}H NMR spectrum (400 MHz, $CDCl_3$) of **2,2′-diOAc**.

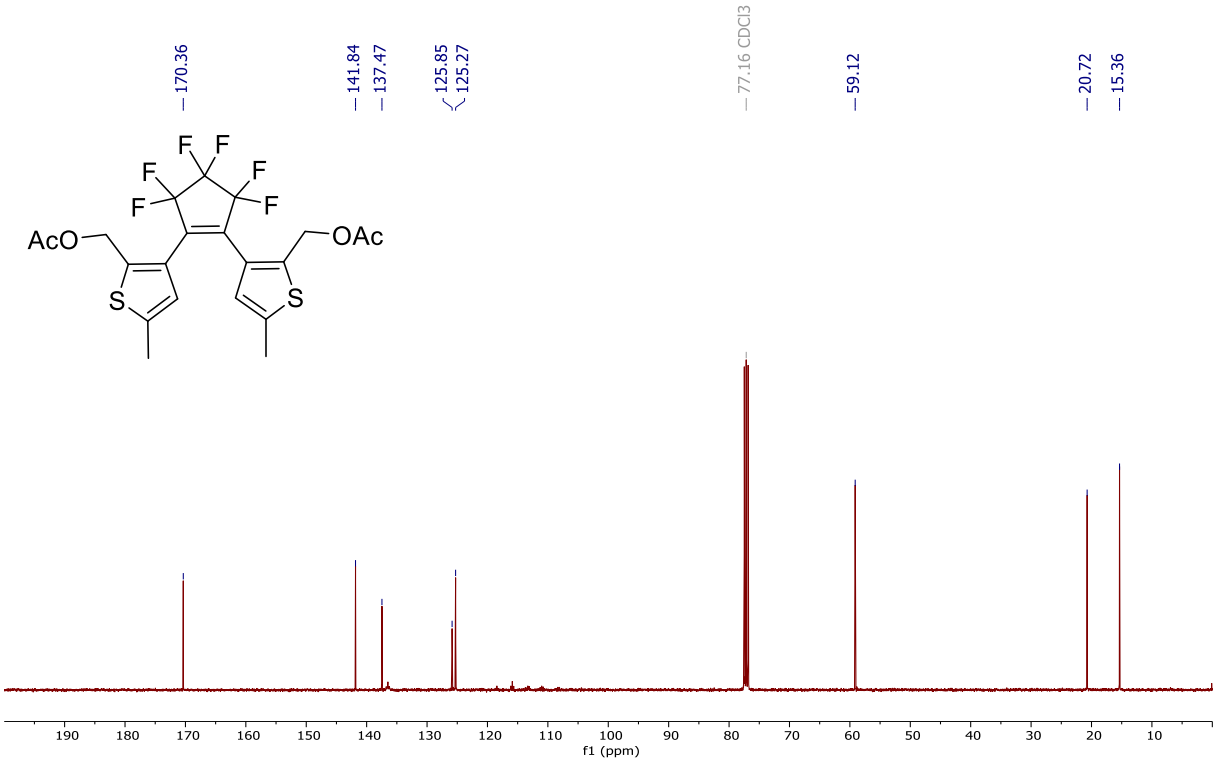

Figure S28. ^{13}C NMR spectrum (100 MHz, $CDCl_3$) of **2,2′-diOAc**.

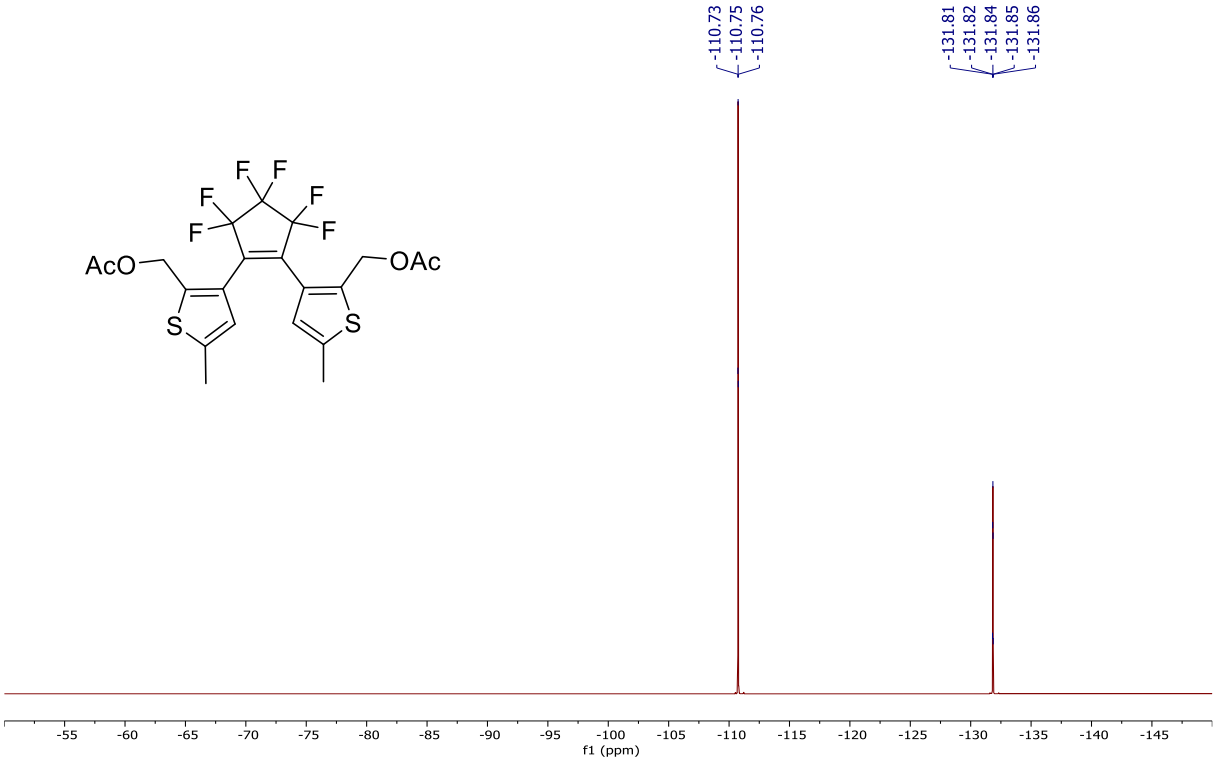

Figure S29. ^{19}F NMR spectrum (377 MHz, $CDCl_3$) of **2,2′-diOAc**.

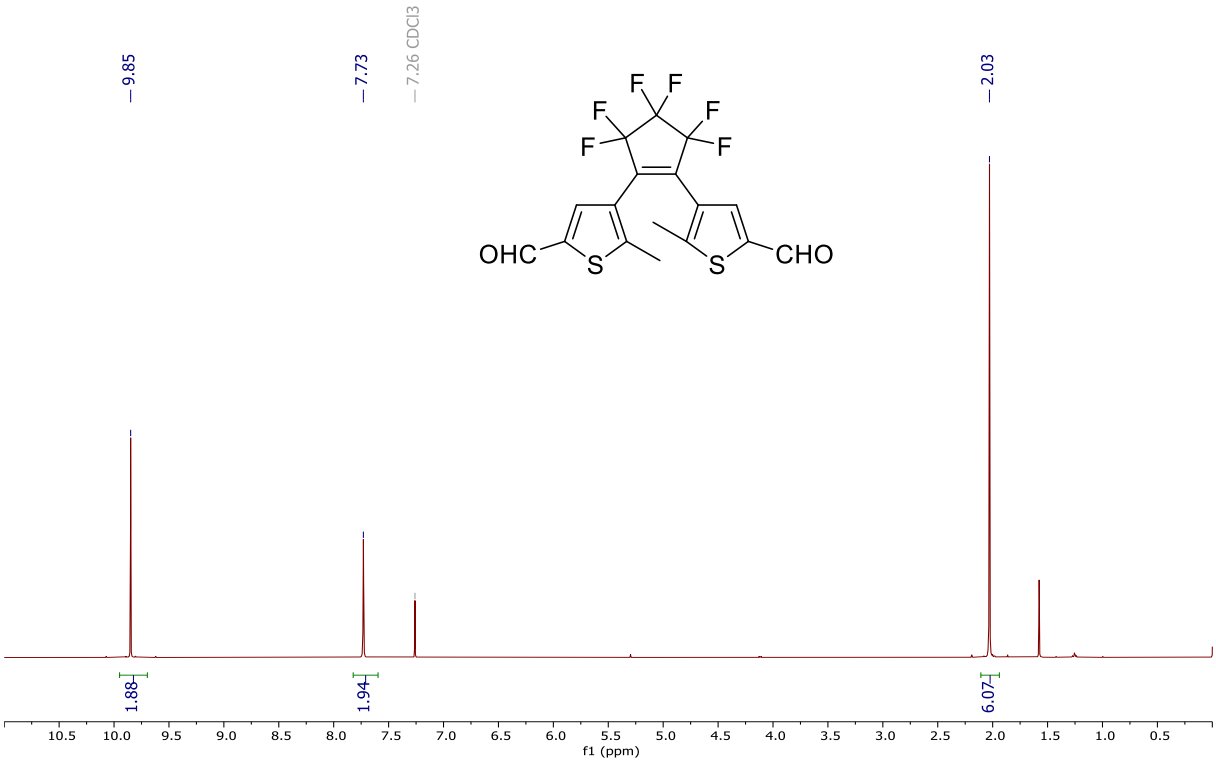

Figure S30. ^{1}H NMR spectrum (400 MHz, $CDCl_3$) of **7**.

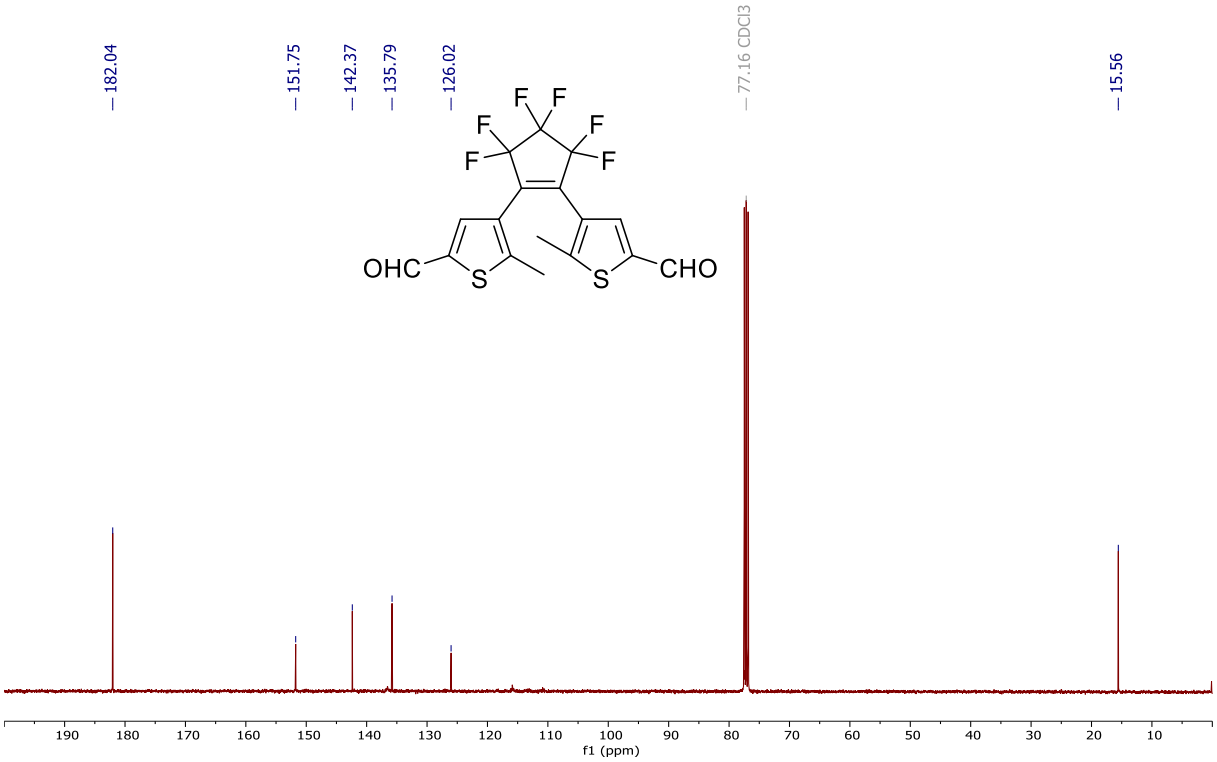

Figure S31. ^{13}C NMR spectrum (100 MHz, $CDCl_3$) of **7**.

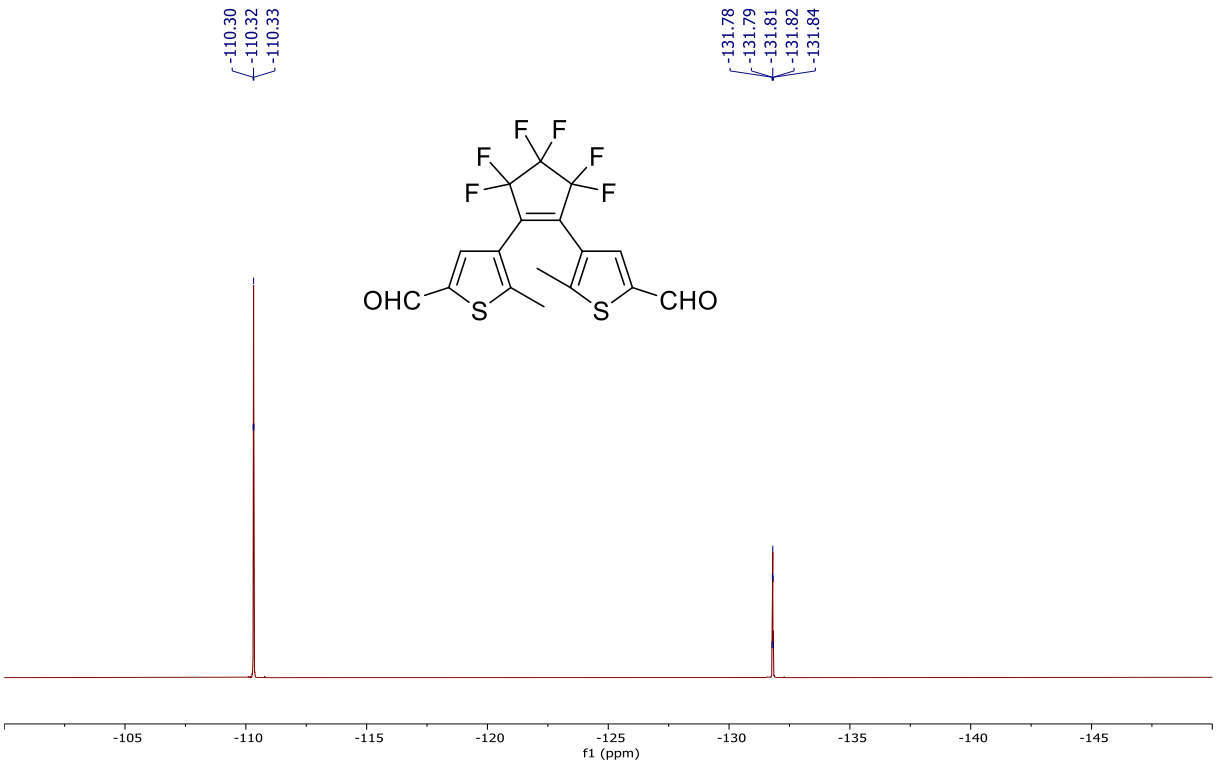

Figure S32. ^{19}F NMR spectrum (377 MHz, $CDCl_3$) of **7**.

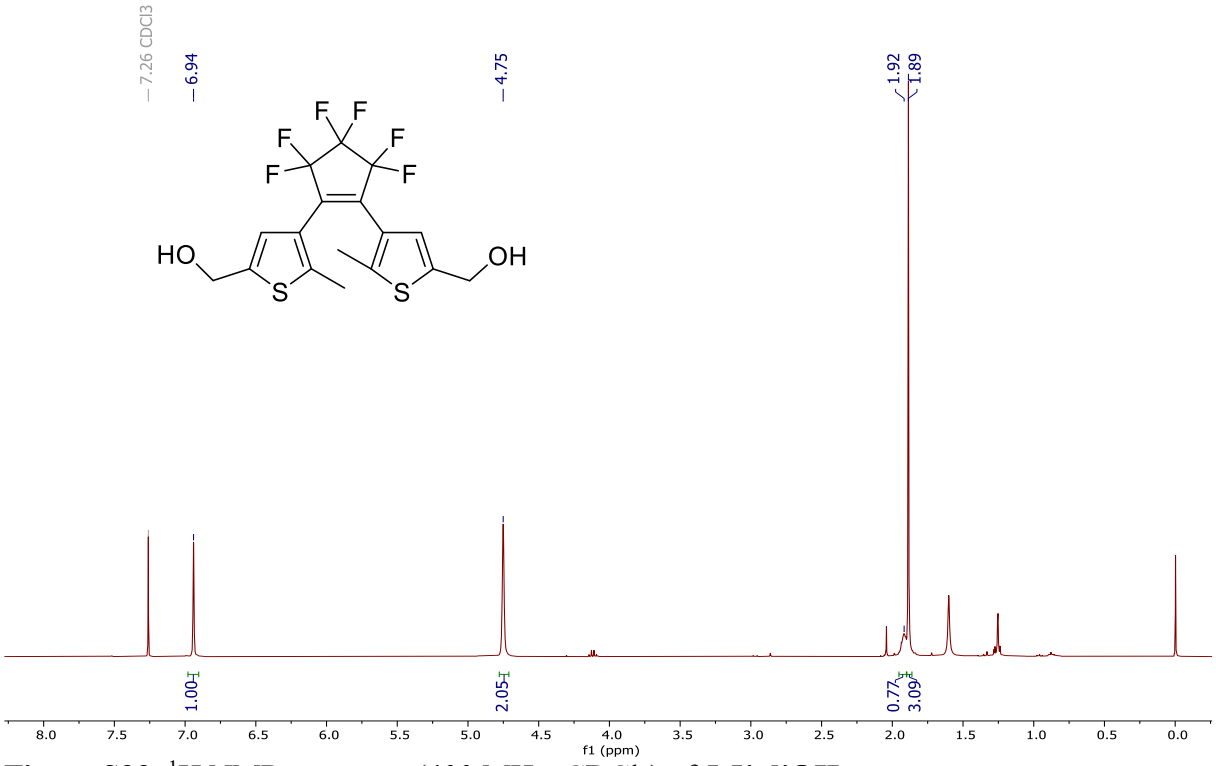

Figure S33. ^{1}H NMR spectrum (400 MHz, $CDCl_3$) of **5,5′-diOH**.

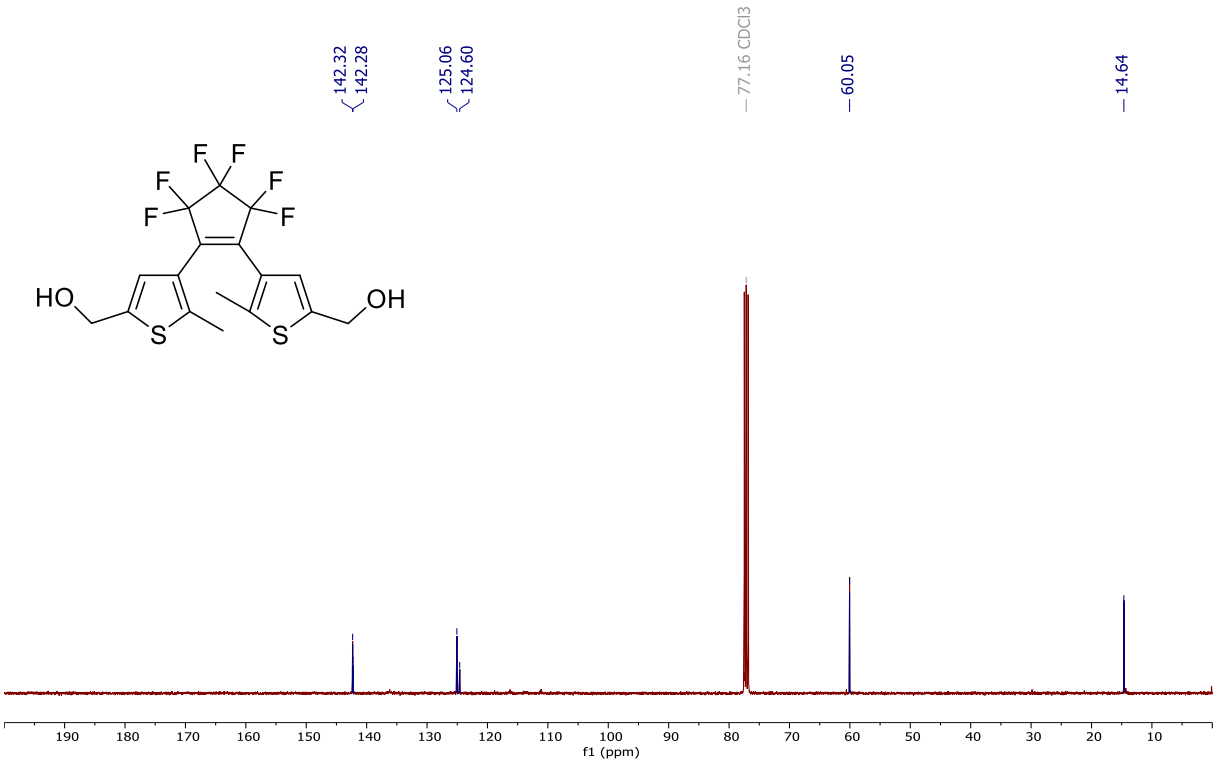

Figure S34. ^{13}C NMR spectrum (100 MHz, $CDCl_3$) of **5,5′-diOH**.

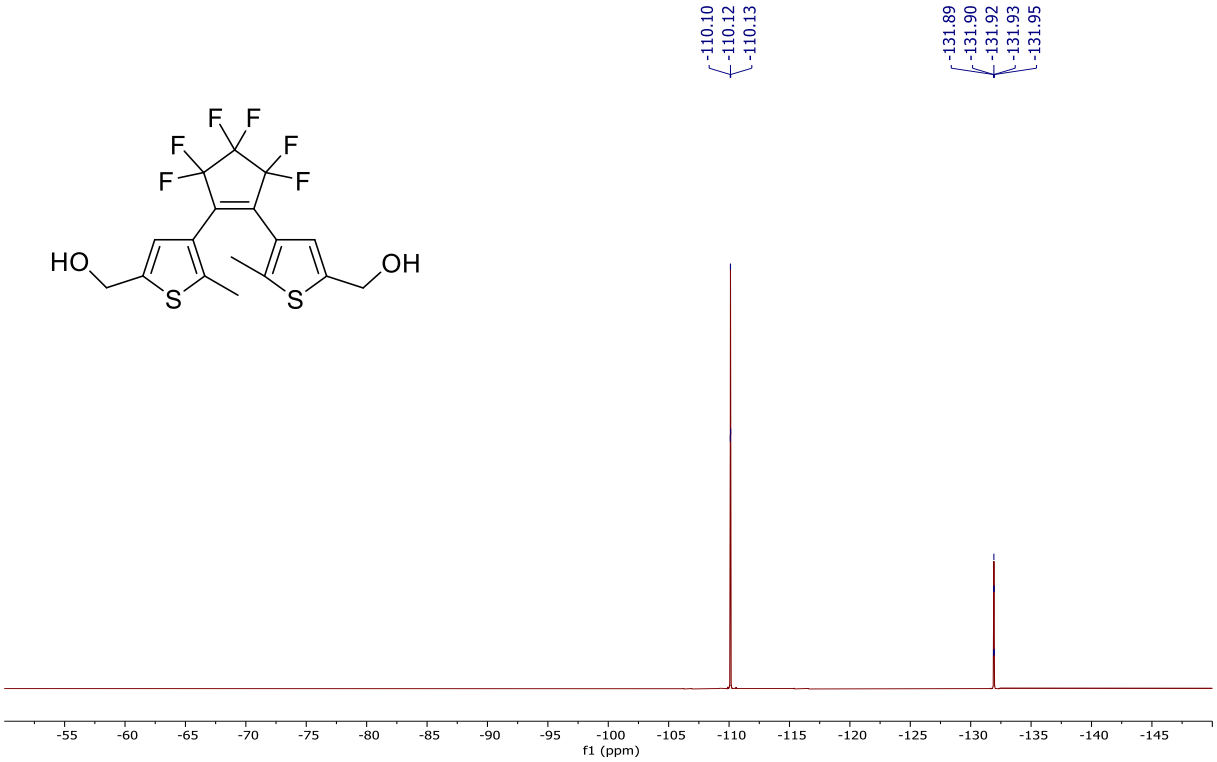

Figure S35. ^{19}F NMR spectrum (377 MHz, $CDCl_3$) of **5,5′-diOH**.

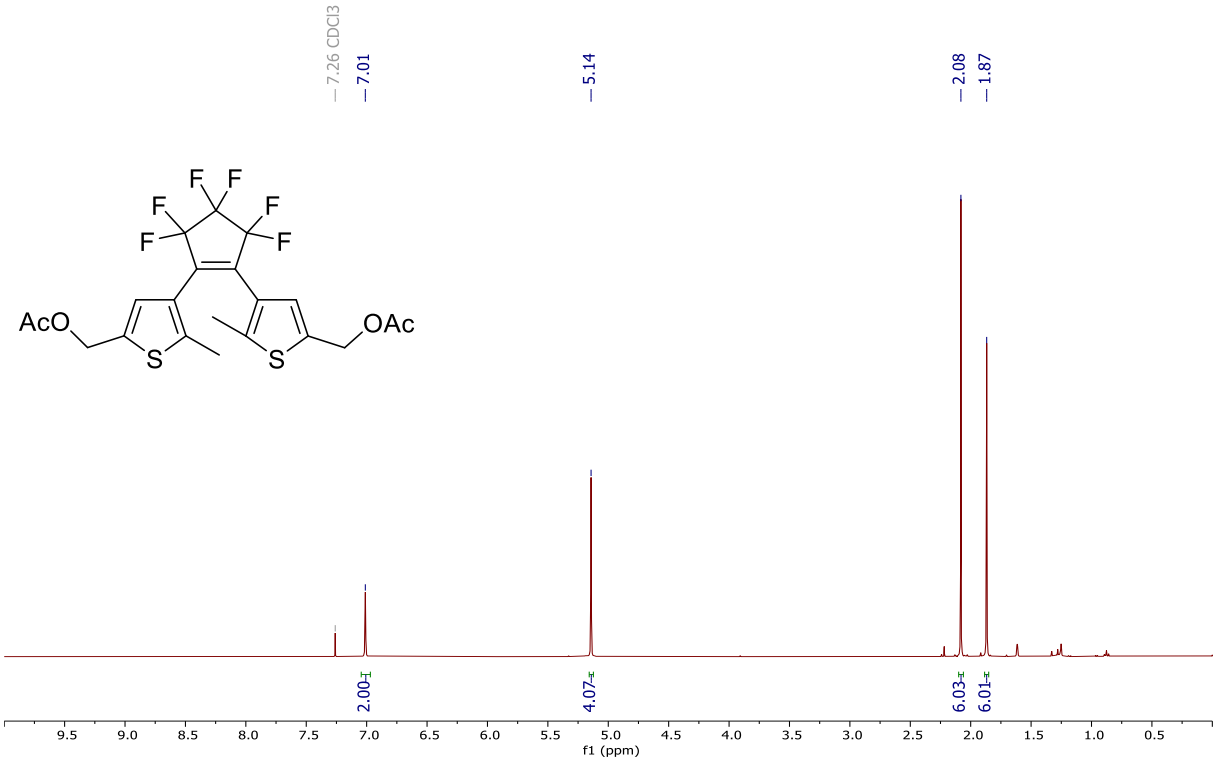

Figure S36. ^{1}H NMR spectrum (400 MHz, $CDCl_3$) of **5,5′-diOAc**.

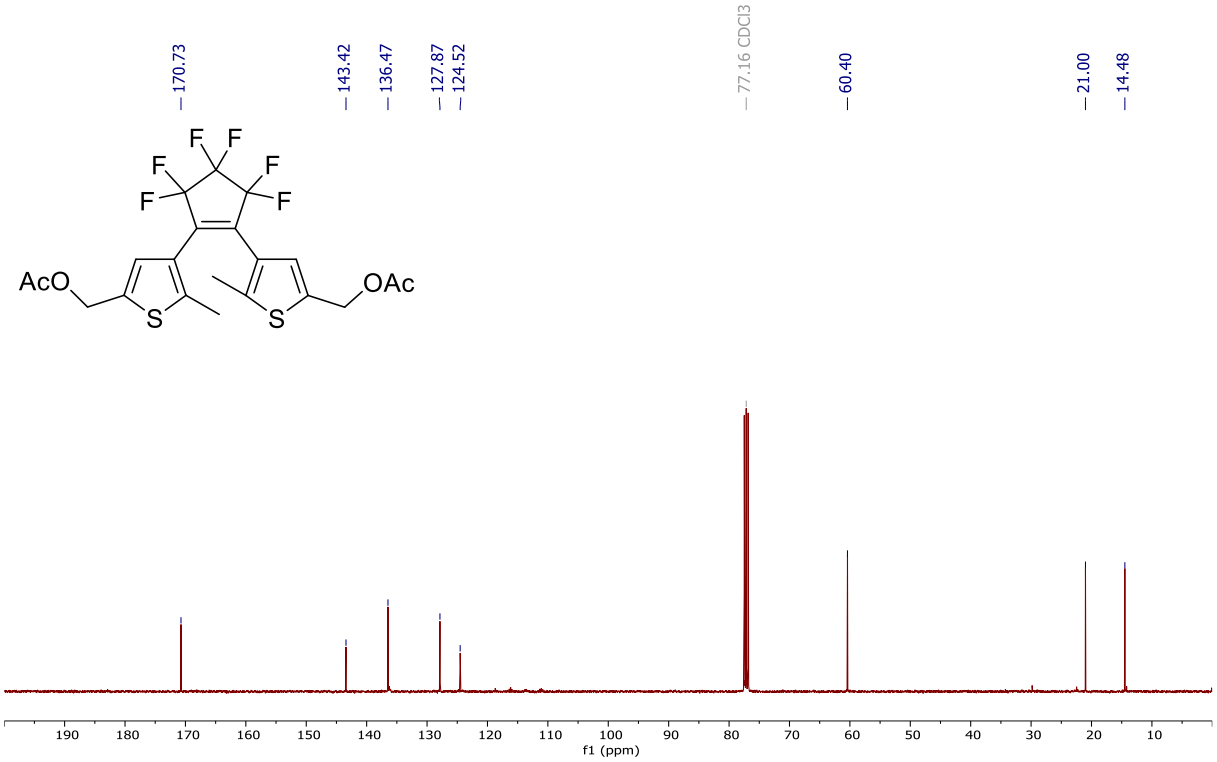

Figure S37. ^{13}C NMR spectrum (100 MHz, $CDCl_3$) of **5,5′-diOAc**.

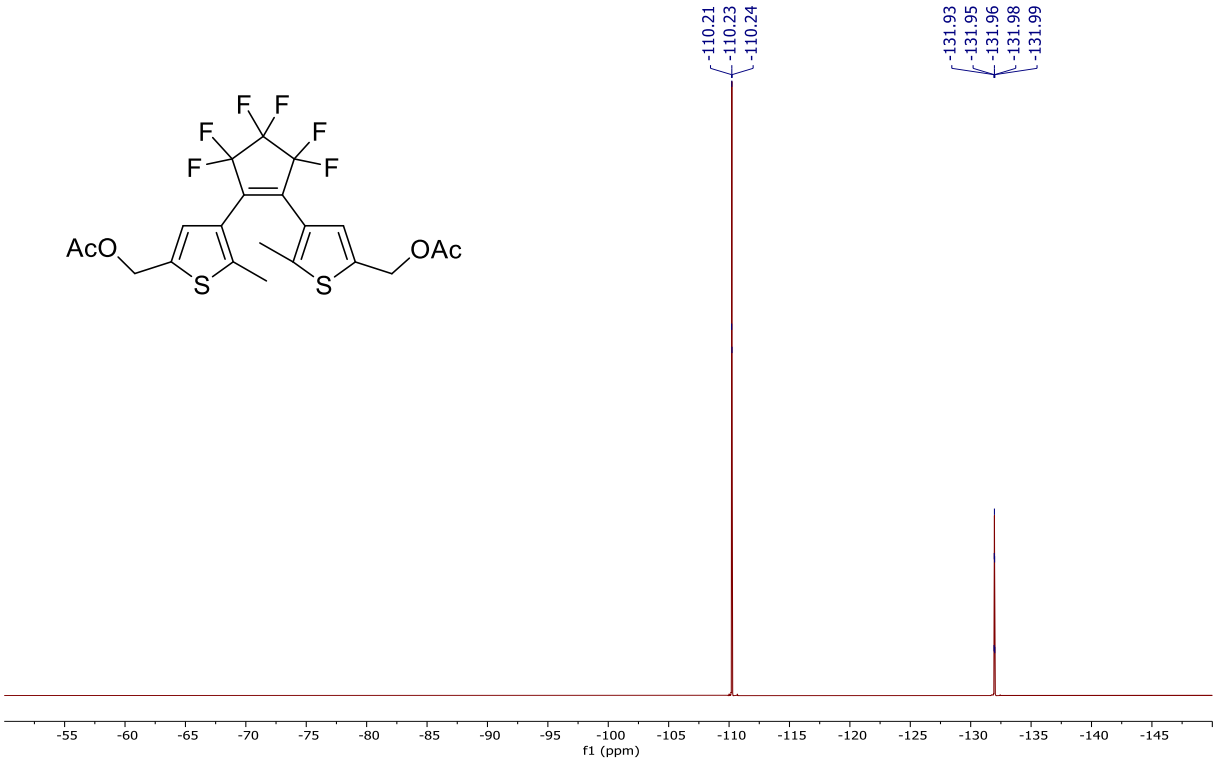

Figure S38. ^{19}F NMR spectrum (377 MHz, $CDCl_3$) of **5,5′-diOAc**.

3. Measurements and Analysis

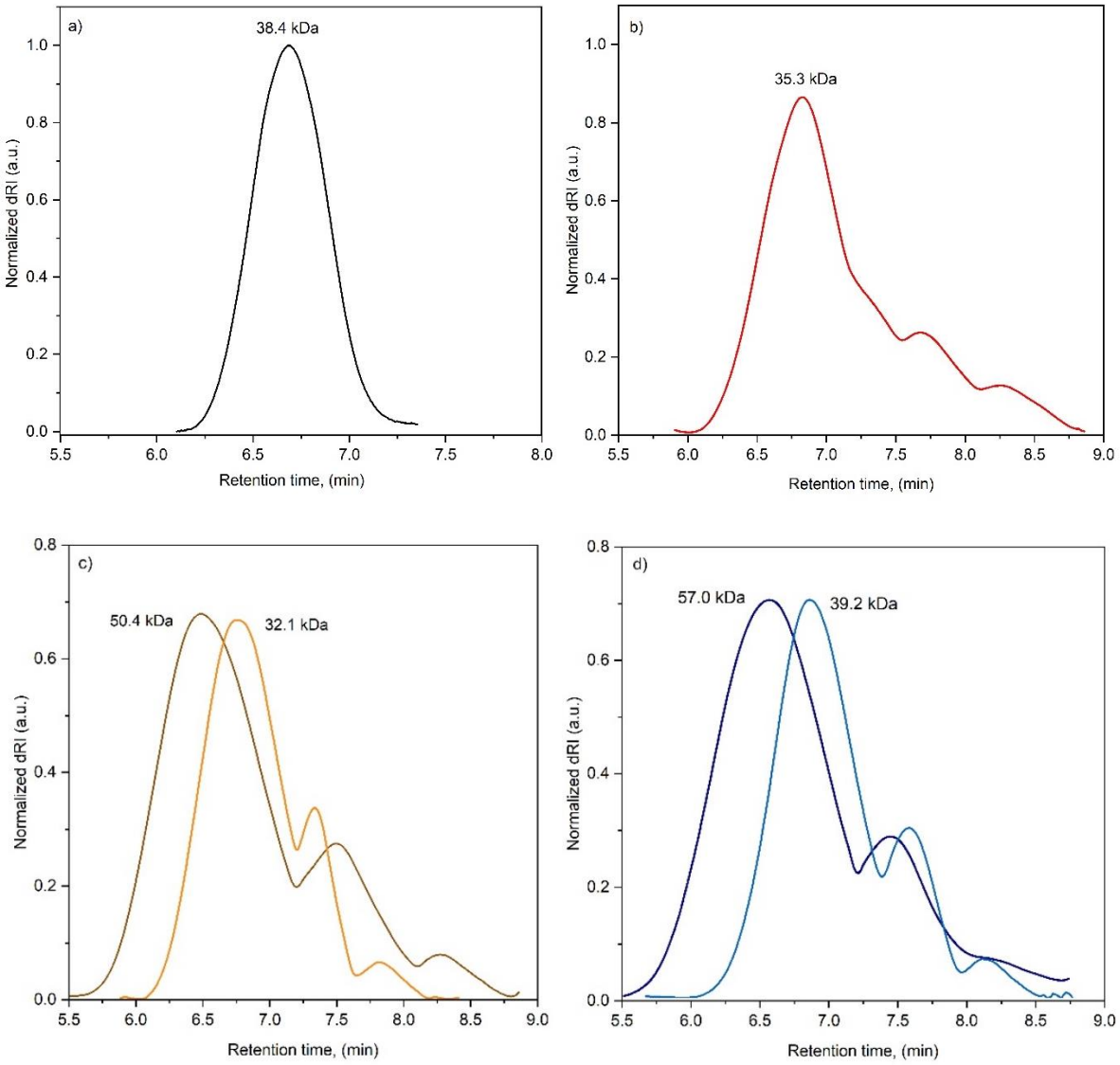

Figure S39. GPC chromatograms of a) poly(ε-caprolactone) without DTE; b) poly(ε-caprolactone) without DTE after 5 [UV-force] cycles of 120 min. each; c) **5,5'-$_{L}$PCL** and **5,5'-$_{M}$PCL** after 5 [UV-force] cycles of 120 min. each; d) **2,2'-$_{L}$PCL** and **2,2'-$_{M}$PCL** after 5 [UV-force] cycles of 120 min. each, showing polymer degradation.

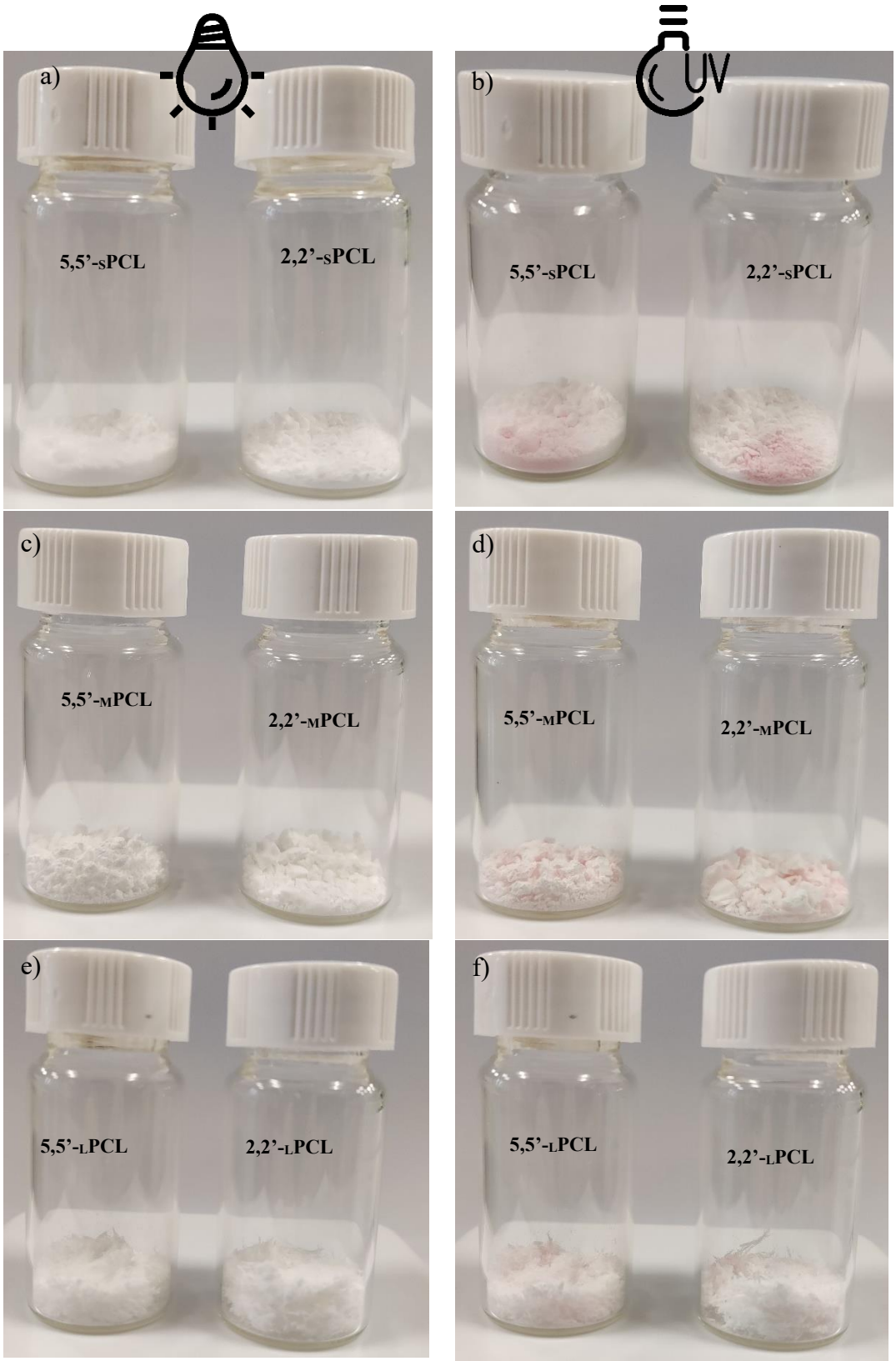

Figure S40. Different molecular weight polycaprolactone polymers with 2,2'-DTE and 5,5'- DTE chromophores: a), b) small; c), d) medium; e), f) large.

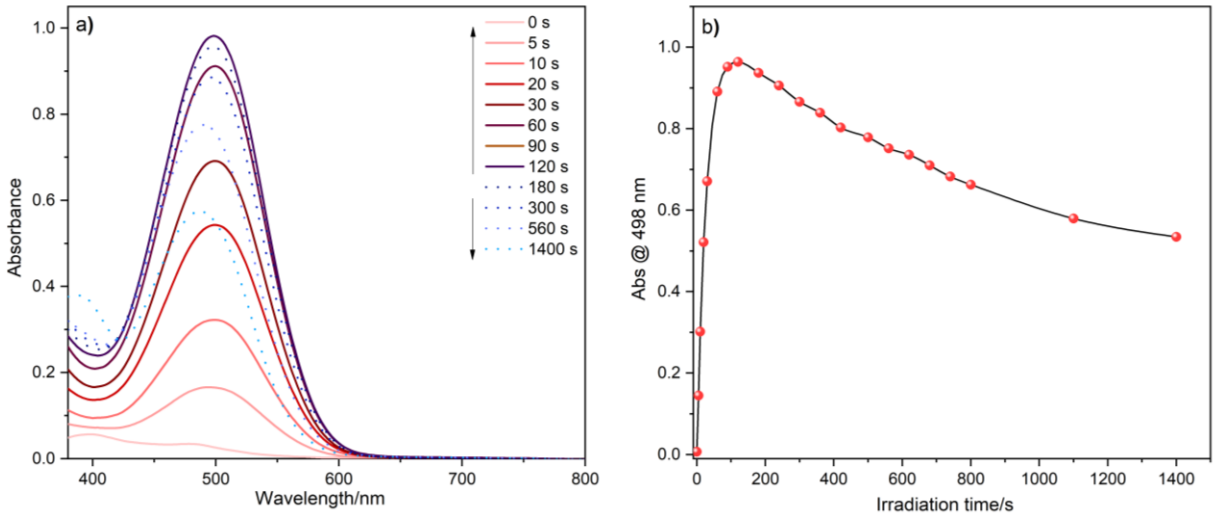

Figure S41. a) UV−vis absorption spectra of **2,2'-ᴍPCL** (1.31 wt% in 1,4 - dioxane). b) UV−vis absorption measurements performed after irradiation by UV light after 0, 5, 10, 20, 30, 60, 90, 120, 180, 300, 560, 1400 s. b) The change at a λ_{max} at 498 nm at different irradiation times.

Figure S42. Color change of the solution of **2,2'-ᴍPCL** in 1,4-dioxane during UV irradiation at different points in time: 0, 5, 10, 20, 30, 60, 90, 120, 180, 300, 560, and 1400 s.

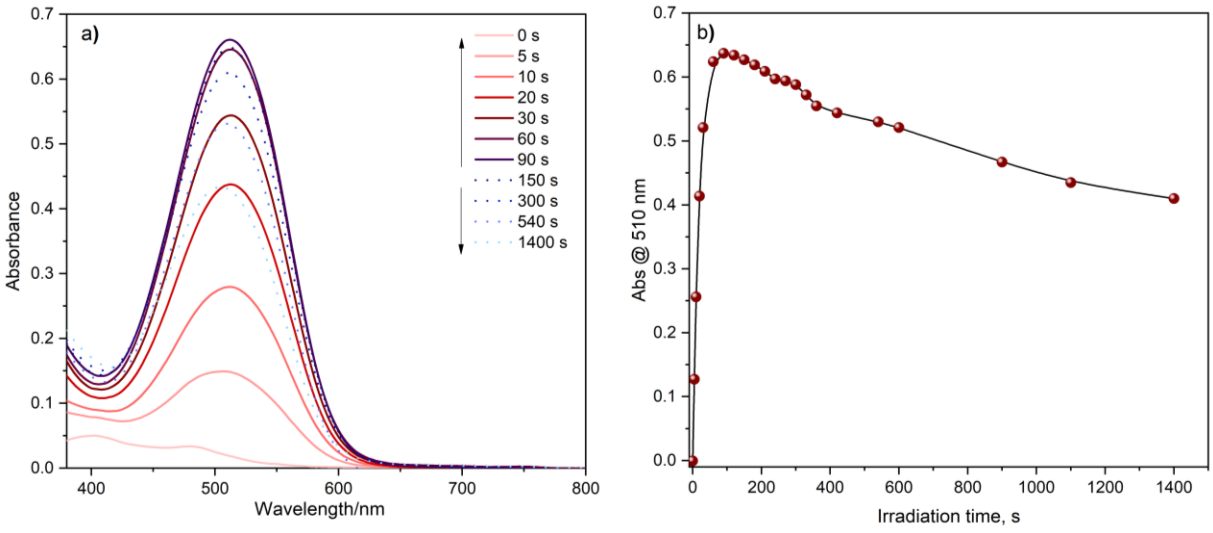

Figure S43. a) UV−vis absorption spectra of **5,5'-ᴍPCL** (1.20 wt% in 1,4 - dioxane). b) UV−vis absorption measurements were performed after irradiation by UV light after 0, 5, 10, 20, 30, 60, 90, 120, 180, 300, 560, 1400 s. b) The change at a λ_{max} at 510 nm at different irradiation times.

Figure S44. Color change of the solution of **5,5'-MPCL** in 1,4-dioxane during UV irradiation at different points in time: 0, 5, 10, 20, 30, 60, 90, 120, 180, 300, 560, and 1400 s.

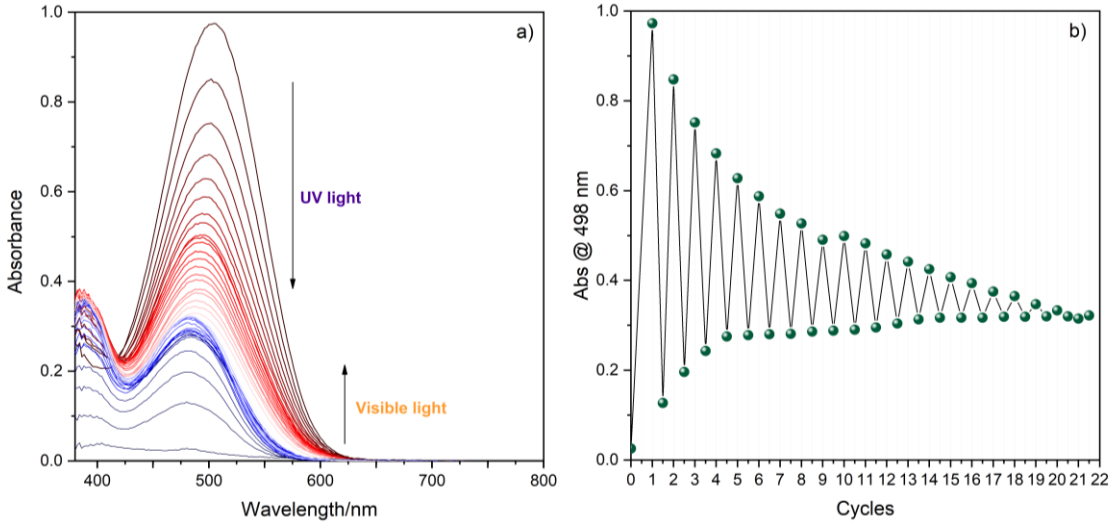

Figure S45. a) UV−vis absorption spectra of **2,2'-MPCL** solutions in 1,4-dioxane (1.31 wt%) under alternating exposure to UV and visible light, fatigue measurement. b) Absorption changes at 498 nm under alternating irradiation with UV and visible light, a λ_{max} at 498 nm. One cycle consists of excitation by UV and quenching by visible light.

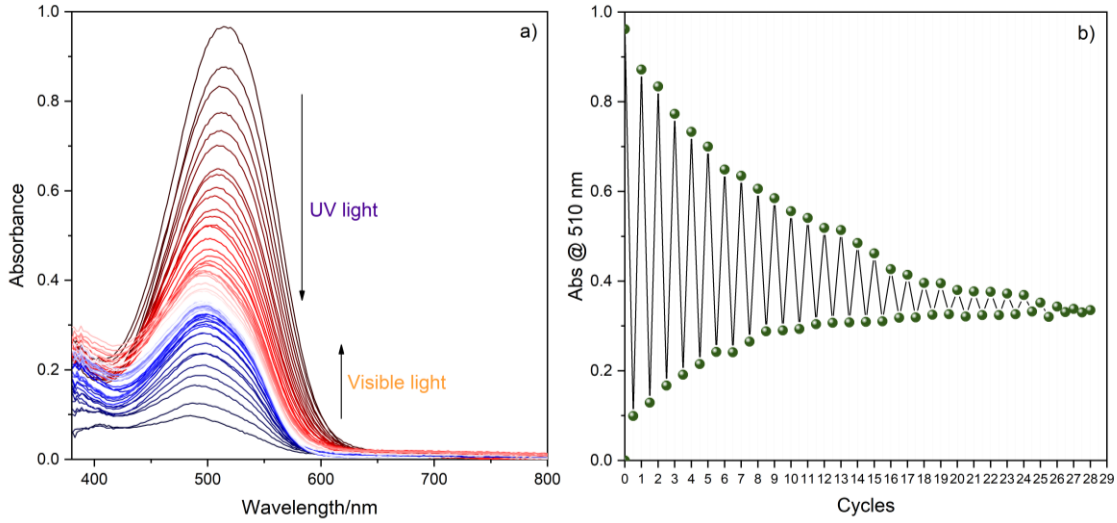

Figure S46. a) UV−vis absorption spectra of **5,5'-MPCL** solutions in 1,4-dioxane (1.20 wt%) under alternating exposure to UV and visible light, fatigue measurement. b) Absorption changes at 510 nm under alternating irradiation with UV and visible light, a λ_{max} at 510 nm. One cycle consists of excitation by UV and quenching by visible light.

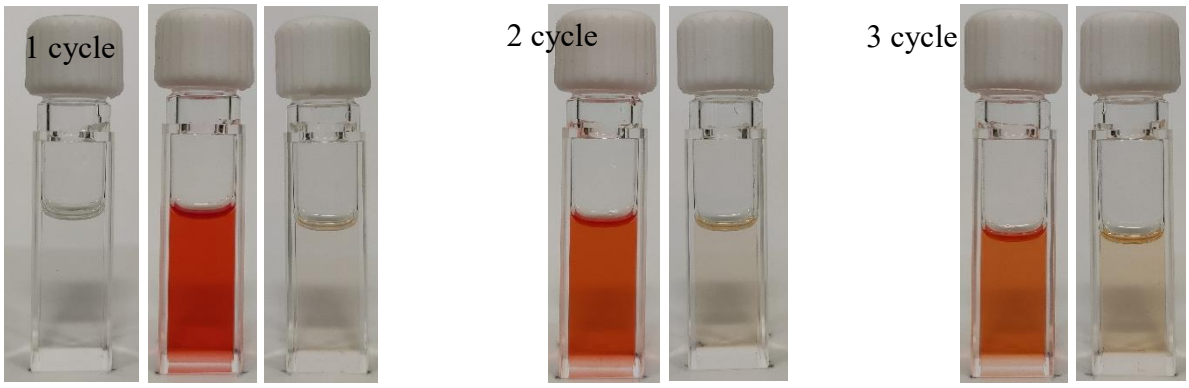

Figure S47. Color change of the solution **2,2'-ᴍPCL** in 1,4-dioxane during 3 cycles of UV irradiation for 2 min and ultrasonication.

Figure S48. Color change of the solution **5,5'-ᴍPCL** in 1,4-dioxane during 3 cycles of UV irradiation for 1.5 min and ultrasonication.

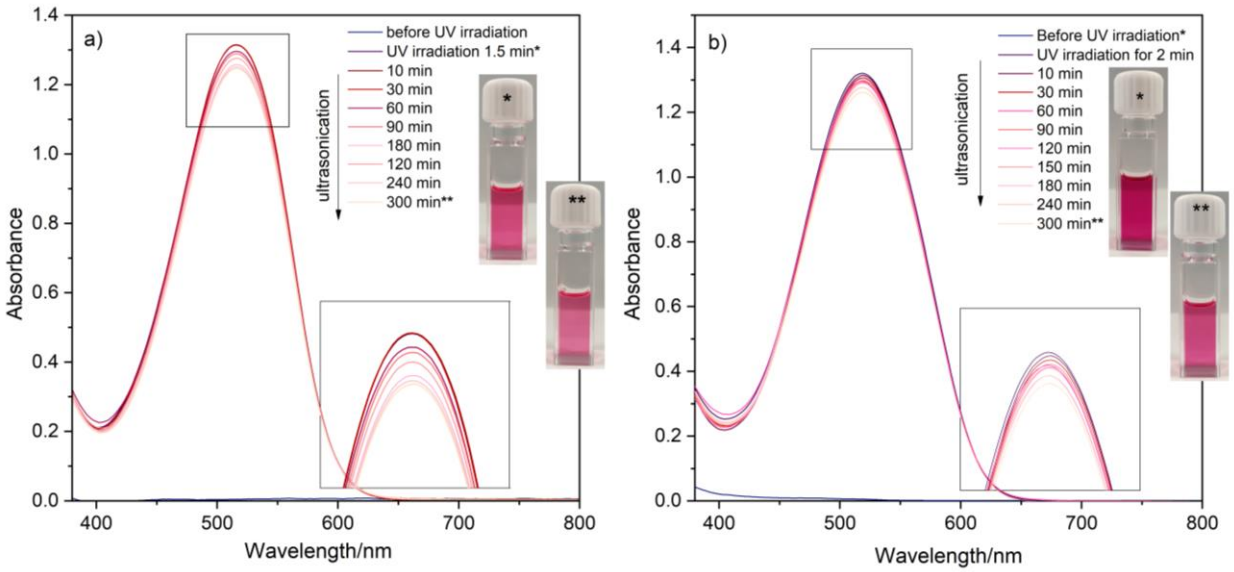

Figure S49. a) UV−vis absorption spectra of control 5,5'-DTE (**5,5'-diOH**) and polymer poly(ε-caprolactone) (1.2 wt% in 1,4-dioxane); 311 nm UV irradiation and subsequent exposure to ultrasound; λ_{max} 510 nm. b) UV−vis absorption spectra of control 2,2'-DTE (**5,5'-diOH**) and polymer poly(ε-caprolactone) (1.31 wt% in 1,4-dioxane). After 311 nm UV irradiation and subsequent exposure to ultrasound; λ_{max} 498 nm.

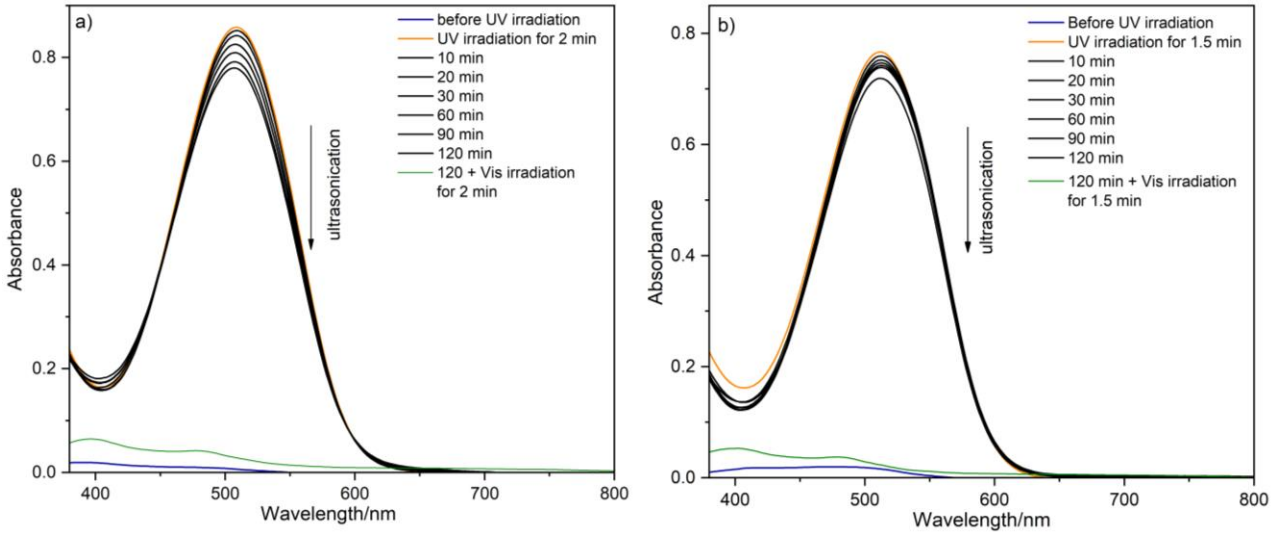

Figure S50. UV−Vis absorption spectra of (a) **2,2'-sPCL** (1.14 wt% in 1,4-dioxane) and (b) **5,5'-sPCL** (1.11 wt% in 1,4-dioxane) before and after 311 nm UV irradiation and subsequent exposure to ultrasound; λ_{max} of 498 nm and 510 nm respectively.

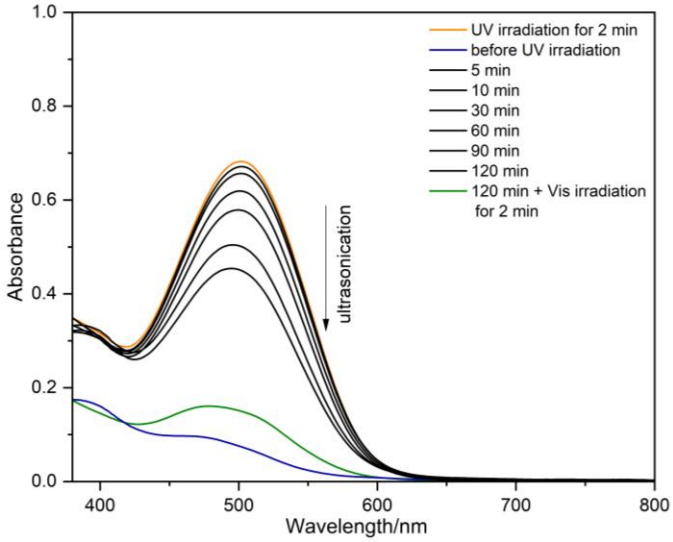

Figure S51. UV−Vis absorption spectra of (a) **2,2'-$_{M}$PCL** (1.31 wt% in 1,4-dioxane) before and after 311 nm irradiation and subsequent exposure to ultrasound, second cycle; λ_{max} = 498 nm.

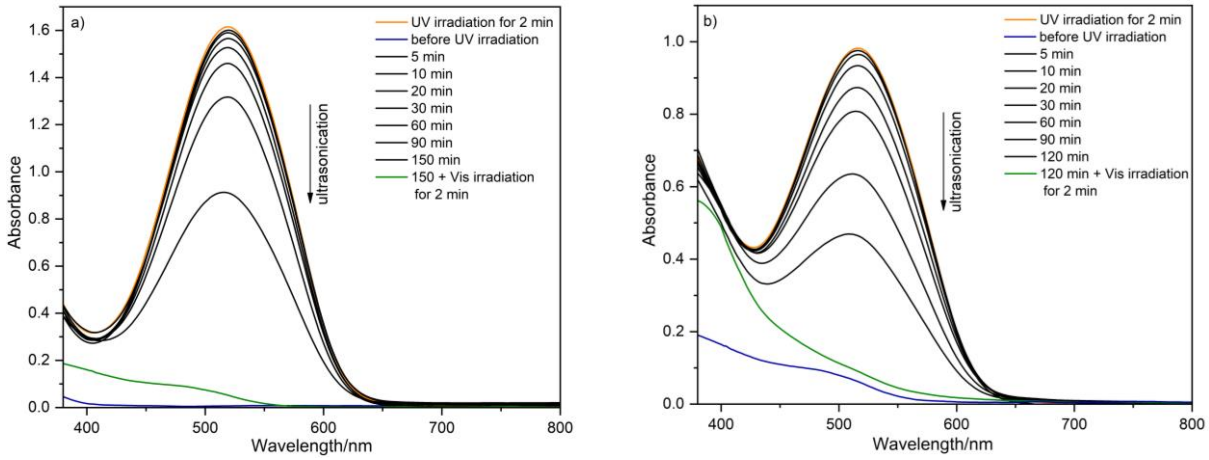

Figure S52. UV−Vis absorption spectra of **2,2'-$_{L}$PCL** (1.34 wt% in 1,4-dioxane) before and after 311 nm irradiation and subsequent exposure to ultrasound, first (a), second (b) cycle; λ_{max} 510 nm.

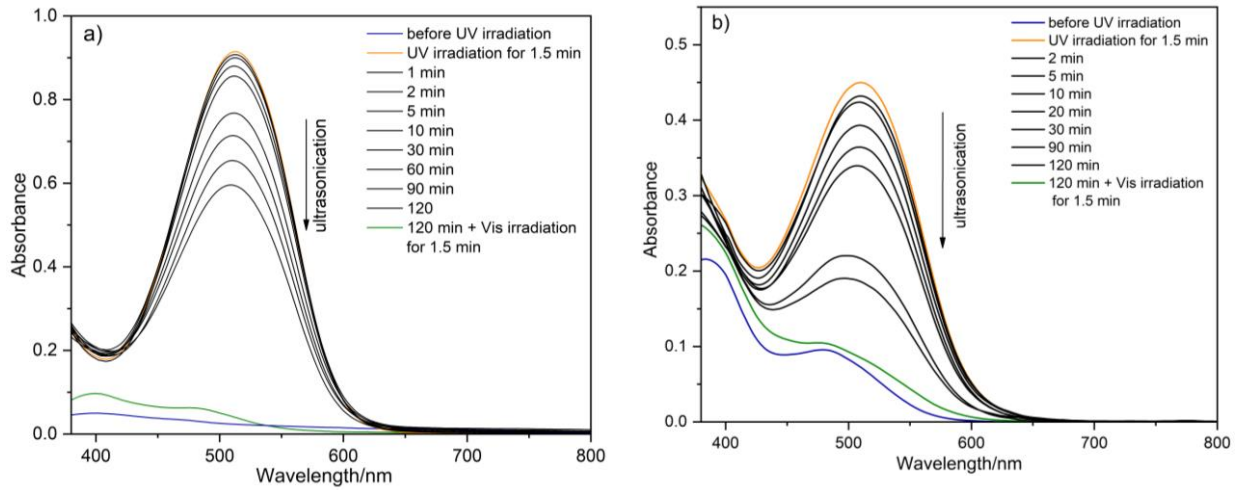

Figure S53. UV−Vis absorption spectra of **5,5'-$_{L}$PCL** (1.27 wt% in 1,4-dioxane) before and after 311 nm irradiation and subsequent exposure to ultrasound, first (a), second (b) cycle; λ_{max} 510 nm.

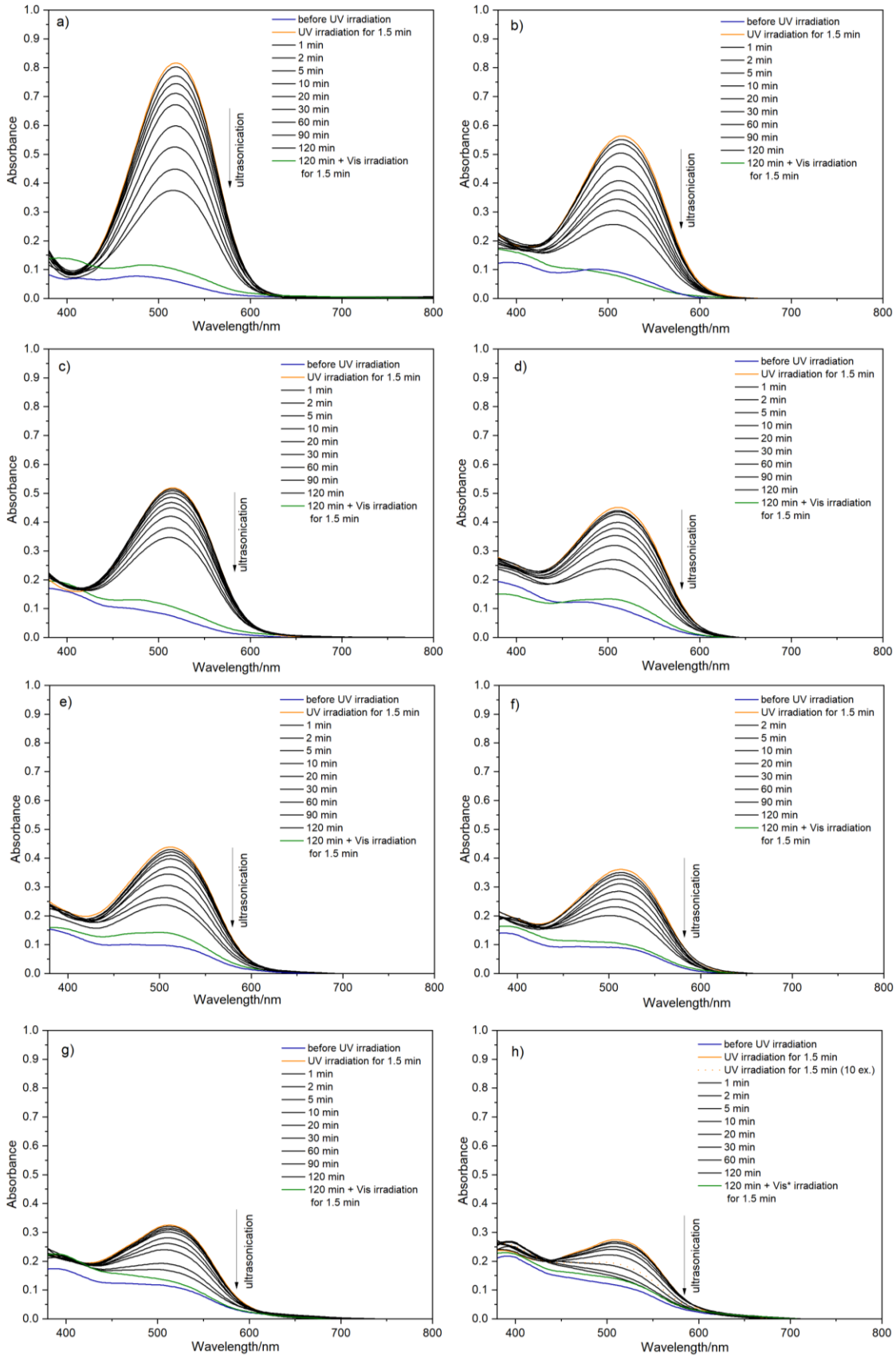

Figure S54. UV−Vis absorption spectra of **5,5'-MPCL** (1.28wt% in 1,4-dioxane) before and after 311 nm irradiation and subsequent exposure to ultrasound, second to ninth cycle (a-h); λ_{max} 510 nm.

References:

1. Neese, F. Software update: the orca program system—version 5.0. *Wiley Interdiscip. Rev. Comput. Mol. Sci.* **12**, e1606 (2022).
2. Bannwarth, C., Ehlert, S. & Grimme. S. GFN2-xTB—An Accurate and Broadly Parametrized Self-Consistent Tight-Binding Quantum Chemical Method with Multipole Electrostatics and Density-Dependent Dispersion Contributions. *J. Chem. Theory Comput.* **15**, 1652-1671 (2019).
3. Neese, F., Wennmohs, F., Becker, U. & Riplinger, C. The ORCA quantum chemistry program package. *J Chem Phys.* **152**, 224108 (2020).
4. Fukagawa, M., Kawamura, I., Ubukata, T. & Yokoyama, Y. Enantioselective Photochromism of Diarylethenes in Human Serum Albumin. *Chem. Eur. J.* **19**, 9434-9437 (2013).
5. Fredrich, S., Bonasera, A., Valderrey, V. & Hecht, S. Sensitive Assays by Nucleophile-Induced Rearrangement of Photoactivated Diarylethenes. *J. Am. Chem. Soc.* **140**, 6432-6440 (2018).
6. Nagorny, S., Weingartz, T., Namyslo, J. C., Adams, J. & Schmidt, A. Correlation between Absorption and Substitution of Photochromic 1,2-Bis(thienyl)ethenes (BTEs) Using Modified Spectroscopic Hammett Equations. *Eur. J. Org. Chem.* **26**, e202200996 (2023).
7. Singh, B., Bankar, S. K. & Ramasastry, S. S. V. Pd-Catalyzed Nazarov-Type Cyclization: Application in the Total Synthesis of β-Diasarone and Other Complex Cyclopentanoids. *Org. Lett.* **24**, 1043-1048 (2022).
8. Majee, D., Ramanauskaite, G. & Presolski, S. Electronic Influences on the Dynamic Range of Photoswitchable Dithienylethene–Thiourea Organocatalysts. *J. Org. Chem.* **88**, 4372-4378 (2023).
9. Maeda, N., Hirose, T., Yokoyama, S. & Matsuda, K. Rational Design of Highly Photoresponsive Surface-Confined Self-Assembly of Diarylethenes: Reversible Three-State Photoswitching at the Liquid/Solid Interface. *J. Phys. Chem.* **120**, 9317-9325 (2016).